Proposal and performance evaluation of a daylighting system composed of concave and convex parabolic mirrors

Tsuji, Yusuke

(Degree)
博士（工学）

(Date of Degree)
2021-03-06

(Date of Publication)
2022-03-01

(Resource Type)
doctoral thesis

(Report Number)
乙第3399号

(URL)
https://hdl.handle.net/20.500.14094/D2003399

神戸大学博士論文

（論文題目）

Proposal and Performance Evaluation of a Daylighting System Composed of Concave and Convex Parabolic Mirrors
（凹側と凸側放物線ミラーで構成された採光システムの提案と性能評価）

2021年1月

（氏名）辻　雄介

Proposal and Performance Evaluation of a Daylighting System Composed of Concave and Convex Parabolic Mirrors

TSUJI, YUSUKE

Department of Architecture, Kobe University

ABSTRACT

We investigate the innovative and revolutionary new-type daylighting system's behaviour, the composed of concave and convex parabolic (CCCP) daylighting system using two-dimensional ray-tracing code. The CCCP system realises to convert parallel light into highly-dense parallel without focal points. The CCCP system has a large amount of possibility to apply. In this paper, first, we explain the feature of the parabolic mirror. The feature is well-known. However, the theoretical framework does not know well. Second, we define the CCCP system and check the geometric feature of it. Third, we introduce the epoch-making new-type daylighting system, the CCCP daylighting system, and investigate its behaviour using two-dimensional ray-tracing simulations. Fourth, we define the illuminance rate and the performance indexes to estimate the daylighting system's performance. Fifth, we check the shape dependence of the CCCP daylight-

ing system and optimise its shape in the range of our numerical calculations. The last, we investigate the CCCP daylighting system's geographic feature using the optimised value in this paper.

CONTENTS

ACKNOWLEDGEMENTS

There are so many people to thank. First, I am deeply grateful to Professor Hirotaka Suzuki, my great supervisor, for all his support during my PhD course. Especially, he supported me not only my research but also my issue. Second, I thank Professor Kenzo Taga and Professor Kimihiro Sakagami for their careful reading and correctly pointing out improvements to my PhD thesis. Third, I am grateful to Professor Naoya Hara to point out my work issues and give me helpful conversations. Finally, I thank all the people who supported me enormously, helped me solving some severe issues and encouraged me to proceed with my PhD course.

1 INTRODUCTION

Daylighting systems are among the most effective sunlight utilisation systems to realise a comfortable lighting environment inside buildings. They conduct sunlight into interior space of buildings. In general, there are two things that the systems should control to adjust their performance: light flow and density. However, it has many difficulties to realise these controls. In this chapter, we explain the background of daylighting systems. After that, we mention the purpose of this thesis.

1.1 Background

One of the primary topics in environmental problems is energy reduction. It has high potential to solve ecological and economic issues. Recently, the powers that be are intensely interested in these issues only to make their powers stronger and become wealthier. In general, these people always make good citizens believe that to save energy is to save the Earth (e.g. Gore 2007). In this thesis, we do not discuss the correctness of environmental issues. We only argue energy reduction for the economy, basically for saving money to live better. Some environmental actions realise to reduce costs (Other ones accomplish to make the power to be wealthier).

One solution to realise energy reduction is to utilise natural energy: such as wind power, geothermal power, solar power. In particular, solar power has great attention in a wide range of fields recently due to low cost and easy installation. For instance, the former prime minister of Japan, Naoto Kan, mentioned in his election campaign, 'Solar energy is free of charge. The Sun never sends us any bills.' Solar energy has an outstanding possibility to solve environmental issues.

1.2   Daylighting Systems

Daylighting systems are one of the most excellent application to utilise solar power inside buildings. They collect natural sunlight, conduct it into interior space of buildings, diffuse it entire space and realise comfortable light environment (e.g. Hansen 2006, Nair et al. 2014).

1.2.1   Three Structural Elements

Daylighting systems are composed of three elements: collectors, conductors and diffusers.

Figure 1.1 shows the components of daylighting systems clearly. The important point of this argument is the components that determine the performance of daylighting systems. It is collectors. Conductors and diffusers are components to lead the sunlight to inside rooms. Therefore, in this paper, we discuss just the design of collectors.
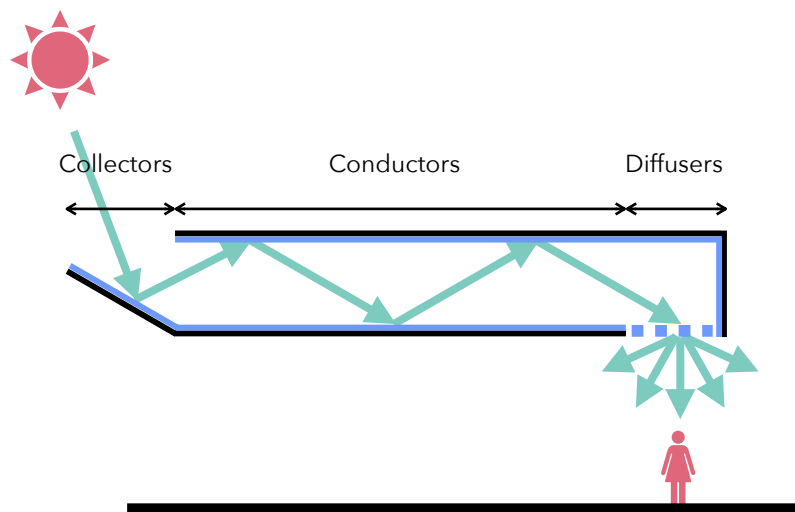
FIGURE 1.1 Daylighting systems have three structural elements. There are three components; collectors, conductors and diffusers.

Collectors

Collectors are the elements that collect and condense the sunlight. The primary purpose of collectors is to send direct and diffuse sunlight to the deep interior of buildings. Collectors are the essential components to improve the performance of daylighting systems. We discuss the classification of collectors deeply in the next section.

Conductors

Conductors realise to transport and extract light. Conductors are also called light ducts or light guides. Light ducts are the equipment that light passes through inside, and the shape is general ducts, like well-known ducts, air ducts. On the other hand, light guides are the equipment whose shape are tubes, like optical fibres. These components lead the sunlight collected by collectors to inside buildings. Besides, conductors have two functions, transporters and extractors.

Diffusers

Diffusers realise to diffuse light. They are the endpoint of daylighting systems. The primary purpose of diffusers is to carry the sunlight into rooms and diffuse condensed light.

In these three elements, collectors are the most important because daylighting systems need to have at least one collector. Besides, collectors determine the greater part of the daylighting systems' performance. Namely, conductors and diffusers are not crucial if thinking the simple daylighting systems.

subsectionTwo Factors to Determine Performance There are two essential factors to improve performance of daylighting systems: a light flow and light density. Daylighting systems could have the best performance to control these two factors properly.

Light Flow

A light flow is an essential factor in reducing the number of reflection. Controlled light flow means collimated light. When the system controls a light flow properly, such a system reduces reflection and minimises the energy loss in transfer. A controlled light flow has a significant advantage because energy loss by reflection is not enough low. In general, the reflectance of mirrors is approximately 90 %. At this reflectance, about 65 % of light energy is disappeared when light reflects ten times. Hence to control a light flow is essential to enhance the performance of daylighting systems.

Light Density

On the other hand, controlled light density realises to produce highly-dense light. When the system controls light density properly, light has a significant advantage at the point of transfer. In general, light transfers to inside buildings with light ducts. Light ducts are the same as, well-known ducts, air ducts except covered with mirrors inside ducts. In general, the smaller diameter of ducts is better due to using space of buildings efficiently. Density controlled light is proper to realise light ducts small.

1.2.2 Light Density and Thermal Problems

We explained two essential factors for daylighting systems: a light flow and light density. The performance of daylighting systems strongly connects both factors. In general, it is not easy to control correctly. One of the most primary reason is thermal problems. When mirrors or lenses correctly control light flow and density, a daylighting system commonly has a focal point(e.g. Tanaka et al. 2012). A focal point is not accepted in architecture because heat melts everything near a focal point (e.g. Suk et al. 2017). The temperature becomes in the order of 10^3 K. Thermal problems are must-be-solved problems in the study of daylighting systems.

1.3 Classification of Collectors

Following previous work (e.g. Hansen 2006, Nair et al. 2014), collectors have three important antagonism classification points: passive systems vs active systems, skylight systems vs sunlight systems and focal systems vs non-focal systems. However, these three-dimensional classification is complicated. Therefore, we introduce a new understandable classification of collectors.

Figure 1.2 shows a new classification of collectors. The vertical line shows energy density, the horizontal one shows a degree of freedom, and the colour shows the collector is the focal system or the non-focal system. This classification is based on the previous discussion of the performance of the daylighting system. The energy density corresponds to light flow and light density controls. The degree of freedom corresponds to the costs of light flow and light density controls. The focal or the non-focal system corresponds to the thermal problems.

Here, we mention one critical condition given in Figure 1.2. In this classification, we ignore the collectors composed of lenses Tripanagnostopoulos et al. (e.g. 2007), Edmonds and Greenup (e.g. 2002) due to several weak points that lenses
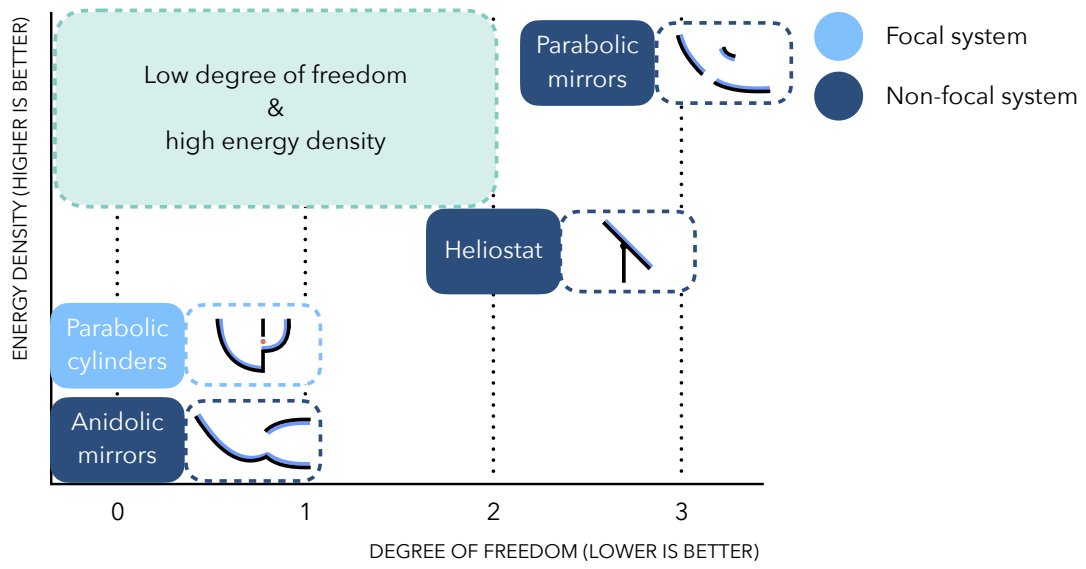
FIGURE 1.2 New classification of collectors.

have. The most significant reason is that the system with lenses cause spectrums. The system should avoid making spectrums when the system uses light as lighting like daylighting systems. Due to the above reasons, we do not include the collectors composed of lenses in the classification shown as Figure 1.2.

The high energy density shows that the daylighting system creates highly-dense light with a few reflections. The few degrees of freedom means the system makes light with small costs for light density control and light flow control. The non-focal system shows that the daylighting system is free of thermal problems. Many researchers approach to realise the high energy density, the few degrees of freedom and non-focal daylighting system (i.e. the system located top-left space in Figure 1.2). However, it is not easy to realise low degrees of freedom and high energy density at the same time due to the restriction of optics.

Next, we introduce several previous works of the daylighting system introduced in Figure 1.2.

1.3.1 Focal System

In general, focal systems should not be used as daylighting systems in architecture due to thermal problems. However, there are several examples of the focal systems, and we introduce briefly.

Parabolic cylinders

The parabolic cylinders system is typically suggested by Tanaka et al. (2012) as the passive skylight focal daylighting system. This system's target is a skylight, so the focal point may not be a significant issue because the focal point does not have enough heat to melt. However, nothing is better due to avoiding the possibility of thermal problems.

1.3.2 Non-focal System

Anidolic Mirrors

The anidolic mirrors system is typically suggested by Courret et al. (1996) as the passive skylight non-focal daylighting system. They introduce their new-type anidolic collector and estimate the performance in a clear sky and an overcast

one. 'anidolic' is a coined word from Greek (an: without, eidolon: image, see (Scartezzini and Courret 2002)). Anidolic systems are composed of non-imaging mirrors and lens.

Heliostats

The heliostats system is typically suggested by Rosemann and Kaase (2005) as the active skylight focal daylighting system. The heliostats system is straightforward. The system has only used one plain mirror with two freedom-degrees. One weak point of this system is that the heliostats control only light flow.

1.3.3 Parabolic mirrors

The parabolic mirrors system is typically suggested by Ullah and Shin (2012). The system is composed of two parabolic mirrors. The work of this thesis strongly connects with their work. We explain the detail of the parabolic mirrors system in Chapter 3.

1.4 Purpose

This thesis suggests the structure composed of concave and convex parabolic mirrors and investigates the geometric feature of this. Next, using this structure, we propose a new-type daylighting system that can realise proper light flow and light density control at the same time without focal points. Finally, we estimate the performance of this new-type system using two-dimensional ray-tracing codes.

Figure 2.4 shows the cross-section image of the CCCP system. This structure can simultaneously control a light flow and density: the structure converts parallel light into a highly dense parallel. The concave mirror converts parallel light from above the system into focusing light by the mirror. Next, the convex mirror realises to convert focusing light from the concave mirror into highly-dense parallel.

This structure's most remarkable feature is that the CCCP system does not have any focal point and realises to convert parallel light into a highly-dense parallel. It means the structure can completely solve thermal problems when this
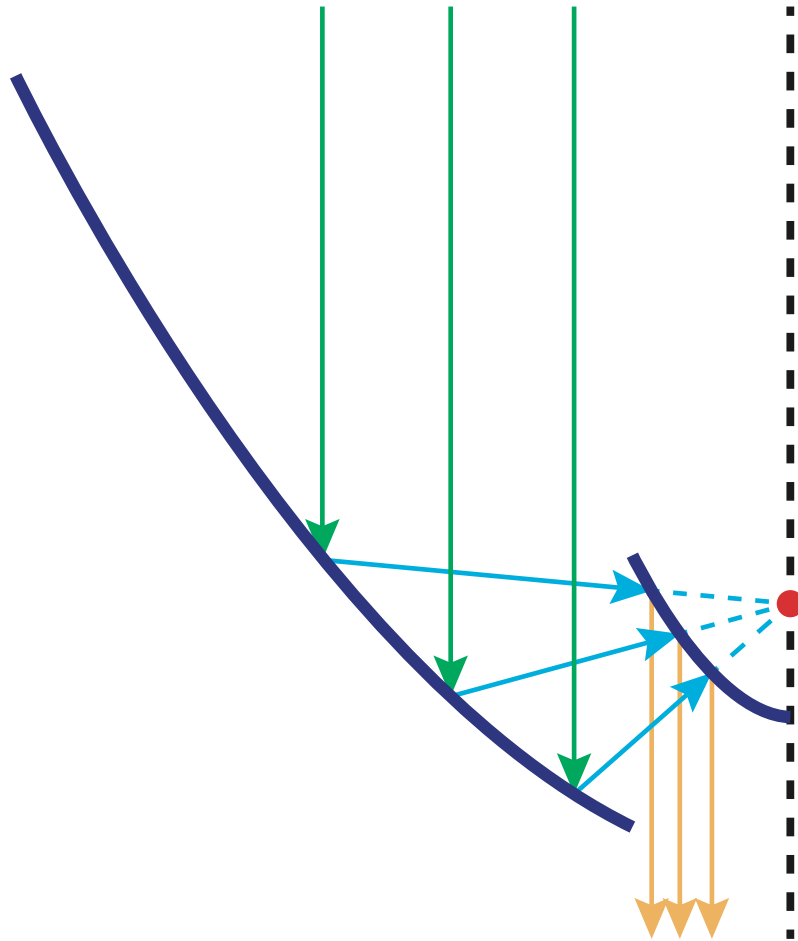
FIGURE 1.3 The cross-section image of the CCCP system. The concave mirror converts parallel light from above the system into focusing light. The convex mirror converts focusing light from the concave mirror into highly-dense parallel light.

INTRODUCTION | 15

structure is applied to daylighting systems.

We summarise our goal of this thesis as below (point 1–3):

1. We comprehend the geometric feature of the new structure composed of concave and convex paraboloidal mirrors.

2. Using new paraboloidal structure, we propose a new-type daylighting system without focal points.

3. We estimate the performance of our system and do practical study for several cases.

A long-time goal is to realise our new-type daylighting system, economical, ecological, safety and efficient system, in real use. This thesis contains the essential discussion of our new-type daylighting systems to utilise the system in the real world.

1.5 Thesis Structure

We organise this thesis as follow: In Chapter 2, we proof the geometric feature of a parabolic mirror, define the CCCP structure and investigate the feature of it. In Chapter 3, we suggest a new-type revolutionary daylighting system, the CCCP daylighting system, set up the mathematical model of it and test using two-dimensional ray-tracing simulations. In Chapter 4, we investigate three types of shape dependence that the CCCP daylighting system has and optimise its shape. In Chapter 5, we find out the CCCP daylighting system's geographic feature using the one-year survey. In Chapter 6, we conclude this thesis.

Figure 1.4 shows the structure of this thesis. from Chapter 2 to Chapter 5 is the main result of this thesis. In particular, composed of concave and convex parabolic (CCCP) structure is the most important and essential keyword in this thesis. This thesis is completely based on the application of this structure.
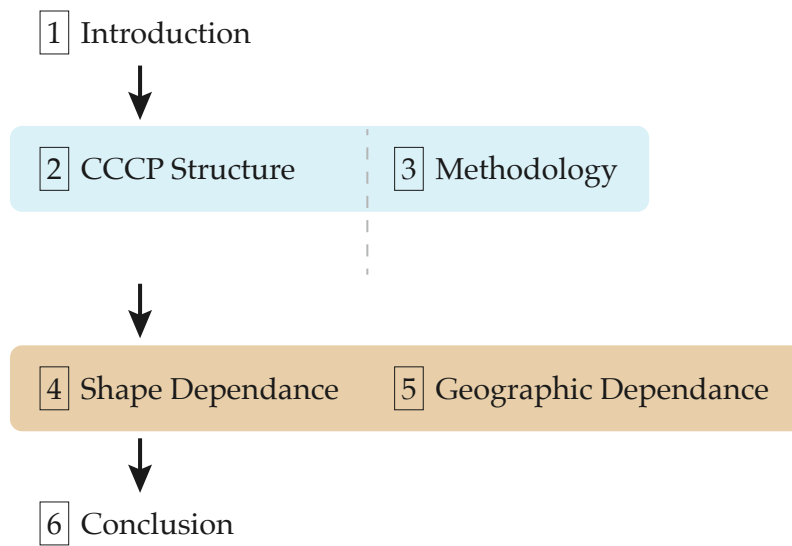
1 Introduction

2 CCCP Structure   3 Methodology

4 Shape Dependance   5 Geographic Dependance

6 Conclusion

FIGURE 1.4 The structure of this thesis.

2 | CCCP Structure

In this chapter, we examine the basic geometric feature of a parabolic mirror. First, we prove that a parabolic mirror is the only solution to convert focusing light into parallel one in plane geometry. Next, we investigate the geometric feature of a parabolic mirror. Finally, we define a new-type parabolic structure, CCCP structure, and explain its feature.

2.1 Basic Theory

It has long been known that the convex side of a parabolic mirror converts focusing light into parallel (e.g. Hecht 1998). Suzuki et al. (2015) explained this feature by solving ordinary differential equations (hereafter, ODE) using a nu-

merical method. Tsuji and Suzuki (2017) found out the analytical solution of this ODE and prove the feature of a parabolic mirror. According to Tsuji and Suzuki (2017), we can get the solution of the ODE as follows.

Figure 2.1 shows the mathematical model that converts focusing light into parallel one. A vector of focusing light v_{in}, a vector of parallel light v_{out} and a tangent vector v_r are defined as

$$v_{in} = \begin{pmatrix} 0 \\ -1 \end{pmatrix}, \tag{2.1}$$

$$v_{out} = \begin{pmatrix} -1 \\ -y/x \end{pmatrix}, \tag{2.2}$$

$$v_r = \frac{\mathrm{d}r}{\mathrm{d}x} = \begin{pmatrix} 1 \\ \mathrm{d}y/\mathrm{d}x \end{pmatrix}. \tag{2.3}$$
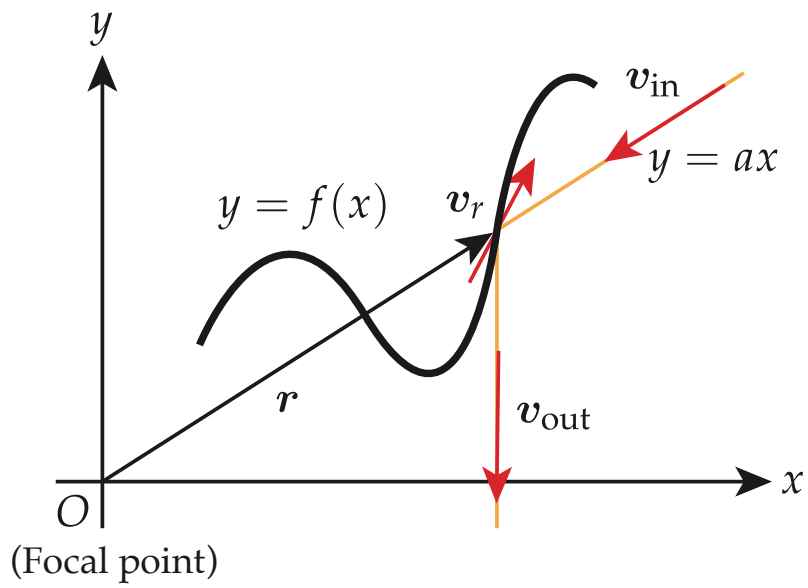
FIGURE 2.1 The mathematical model that converts focusing light into parallel one. v_{in} is a vector of focusing light. v_{out} is a vector of parallel one. $f(x)$ converts v_{in} into v_{out}. v_r is a tangent vector.

Here, we use the definition of an inner product:

$$\cos \theta_{\text{in}} = \frac{\boldsymbol{v}_r \cdot (-\boldsymbol{v}_{\text{in}})}{v_r v_{\text{in}}}, \tag{2.4}$$

$$\cos \theta_{\text{out}} = \frac{\boldsymbol{v}_r \cdot (-\boldsymbol{v}_{\text{out}})}{v_r v_{\text{out}}}, \tag{2.5}$$

where, θ_{in} is the incident angle. θ_{out} is the reflection angle. Using equations (2.1)–(2.5) and the relationship between the incident angle and the reflection angle (i.e. $\cos \theta_{\text{in}} = \cos \theta_{\text{out}}$), we get the ODE that converts focusing light into parallel one:

$$x + 2y\frac{dy}{dx} - x \left(\frac{dy}{dx}\right)^2 = 0. \tag{2.6}$$

Here, we deformation equation (2.6):

$$\frac{dy}{dx} = -\frac{1}{y/x - \sqrt{1 + (y/x)^2}}, \tag{2.7}$$

where, we call this form the homogeneous differential equation. In general, we can get the general solution of this ODE. To solve equation (2.7), we transform variables into $q = y/x$. We get

$$y = qx, \tag{2.8}$$

$$\frac{dy}{dx} = x\frac{dq}{dx} + q. \tag{2.9}$$

Here, we substitute equation (2.8)–(2.9) for equation (2.7):

$$\frac{q - \sqrt{1 + q^2}}{q\sqrt{1 + q^2} - (1 + q^2)} \mathrm{d}q = \frac{1}{x}\mathrm{d}x. \tag{2.10}$$

Here, we call this form the separation of variables. We transform the left side of equation (2.10):

$$\frac{q - \sqrt{1 + q^2}}{q\sqrt{1 + q^2} - (1 + q^2)} = \frac{q - \sqrt{1 + q^2}}{\sqrt{1 + q^2}(q - \sqrt{1 + q^2})}$$

$$= \frac{1}{\sqrt{1 + q^2}}. \tag{2.11}$$

We substitute (2.10) for equation (2.11):

$$\frac{1}{\sqrt{1 + q^2}}\mathrm{d}q = \frac{1}{x}\mathrm{d}x, \tag{2.12}$$

where, we integrate equation (2.12). We get

$$\log\left|q + \sqrt{q^2 + 1}\right| = \log|x| + C. \tag{2.13}$$

Here, C is an integration constant. We deformation equation (2.13):

$$\log\left|\frac{q + \sqrt{q^2 + 1}}{x}\right| = C. \tag{2.14}$$

Here, we use the definition of the logarithm $a^p = M$,

$$\frac{q + \sqrt{q^2 + 1}}{|x|} = e^C.$$ (2.15)

Here, we define $K = e^C > 0$. Hence,

$$\sqrt{q^2 + 1} = K|x| - q.$$ (2.16)

Here, we separate equation (2.16) into the positive case and the negative case to expand a variable $|x|$. At first, we consider the positive case (i.e. $x \geq 0$). We square both sides of equation (2.16) and arrange the equation:

$$K^2 x^2 - 2Kqx - 1 = 0.$$ (2.17)

Using equation (2.8) and (2.17), we get

$$y = \frac{1}{4p}x^2 - p.$$ (2.18)

Here, we put $K = (1/2)p$. Equation (2.18) shows the parabolic equation that has a focal point at the origin of coordinates. With same method, we solve the negative

case (i.e. $x < 0$). Finally we get

$$y = \begin{cases} \dfrac{1}{4p}x^2 - p, & (x \geq 0) \\ \\ -\dfrac{1}{4p}x^2 + p. & (x < 0) \end{cases} \tag{2.19}$$

Here, p is the distance from the focal point of the defined parabola.

Figure 2.2 shows the result of equation (2.19). In both cases, focusing light is converted into parallel. However, there is a great difference between the positive case and the negative one. In the positive case (i.e. $x \geq 0$), the convex parabola converts focusing light into parallel before passing through a focal point. In the negative case (i.e. $x < 0$), the concave parabola converts focusing light into parallel after passing through a focal point. It is important to avoid passing through a focal point due to thermal problems. The positive case shows the possibility of daylighting systems without focal points.

Here, we check the case that $y = mx$ is a solution. The reason that we should
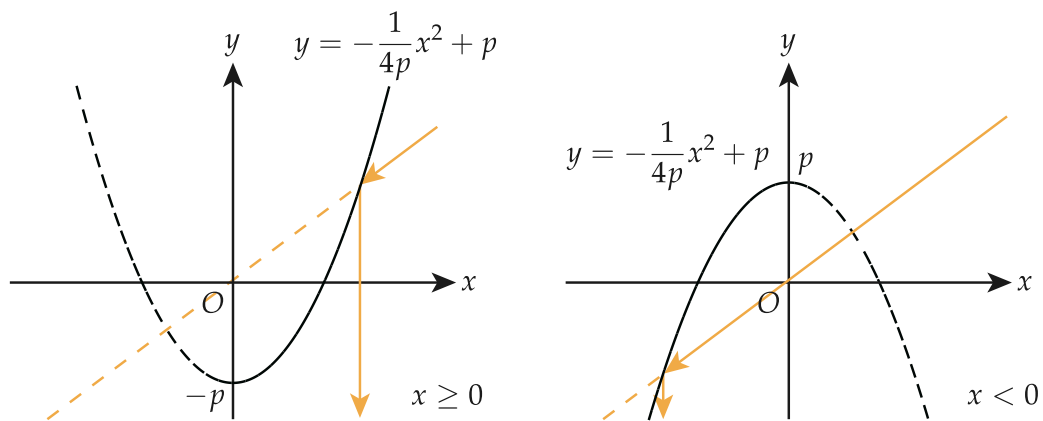
FIGURE 2.2 The result of equation (2.19). The left panel is the case of $x \geq 0$. The right panel is the case of $x < 0$. Equation (2.19) converts focusing light into parallel one in both cases. However, the left panel converts before passing through a focal point. The right panel converts after passing through a focal point.

check this case is the separation of variables could not be applied for $y = mx$. Namely, when $y = mx$ is a solution, we get $q = y/x = m$. Therefore, we need to consider the case of $y = mx$. Here, we substitute $y = mx$ for equation (2.7):

$$
\begin{aligned}
m &= -\frac{1}{m - \sqrt{1+m^2}} \\
&= m + \sqrt{1+m^2}.
\end{aligned}
\tag{2.20}
$$

Hence, we get $m = \pm i$. However, this is an imaginary root. Therefore, we get that $y = mx$ cannot be the solution of equation (2.6).

2.2 Geometric Feature

As a result of Equation (2.6), we get two types of a parabolic mirror to convert focusing light into parallel. However, this feature is also proved using the geometric method. This comprehension is intuitive and understood clearly and obviously.

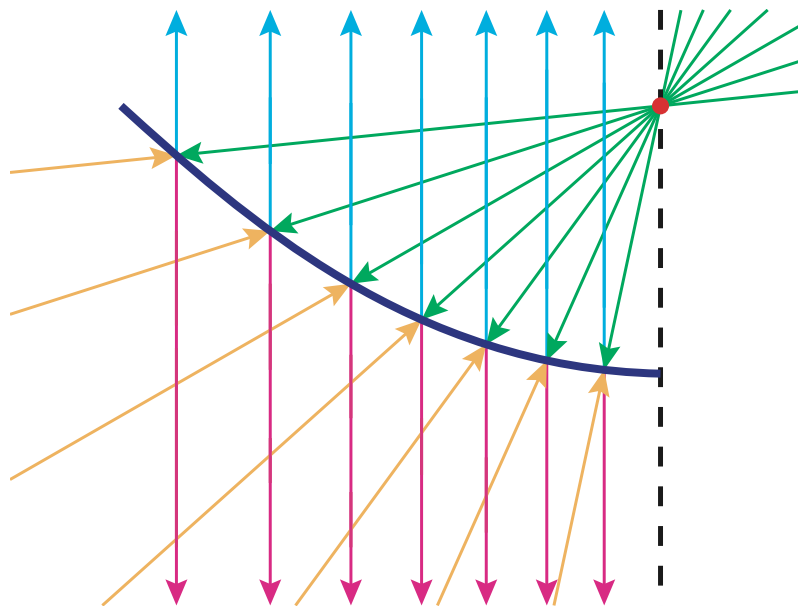Figure 2.3 shows the geometric feature to convert focusing light into par-

FIGURE 2.3 A geometric image to convert focusing light into parallel. The concave side converts focusing light into parallel one after passing through a focal point. The convex side converts focusing light into parallel lights before passing through a focal point.

allel one. The concave side corresponds to the negative case (i.e. $x < 0$) in equation (2.19). The convex side corresponds to the positive case (i.e. $x \geq 0$) in equation (2.19). The most important feature of Figure 2.3 is the convex side. It seems strange. However, it is a completely natural feature in geometry. This feature's correctness can be proved using several easy and well-known theories of geometry and physics (law of reflection and vertical angles).

2.3 CCCP Structure

In general, when a parabolic structure is used to condense light, some focal points appear. Focal points are not preferred when a parabolic structure is used to condense light. The reason that focal points should be avoided is they caused thermal problems. To avert heat problems, we introduce a new-type structure using parabolic structure, the CCCP structure. We discussed the convex side of parabola convert focusing light into parallel one before passing through the focal point. Using this feature and concave and convex side of a parabola, we introduce a new-type structure to convert parallel light into a highly-dense parallel. Using one concave side of a parabola and one convex side of it, we realise to convert parallel light into a highly-dense parallel.
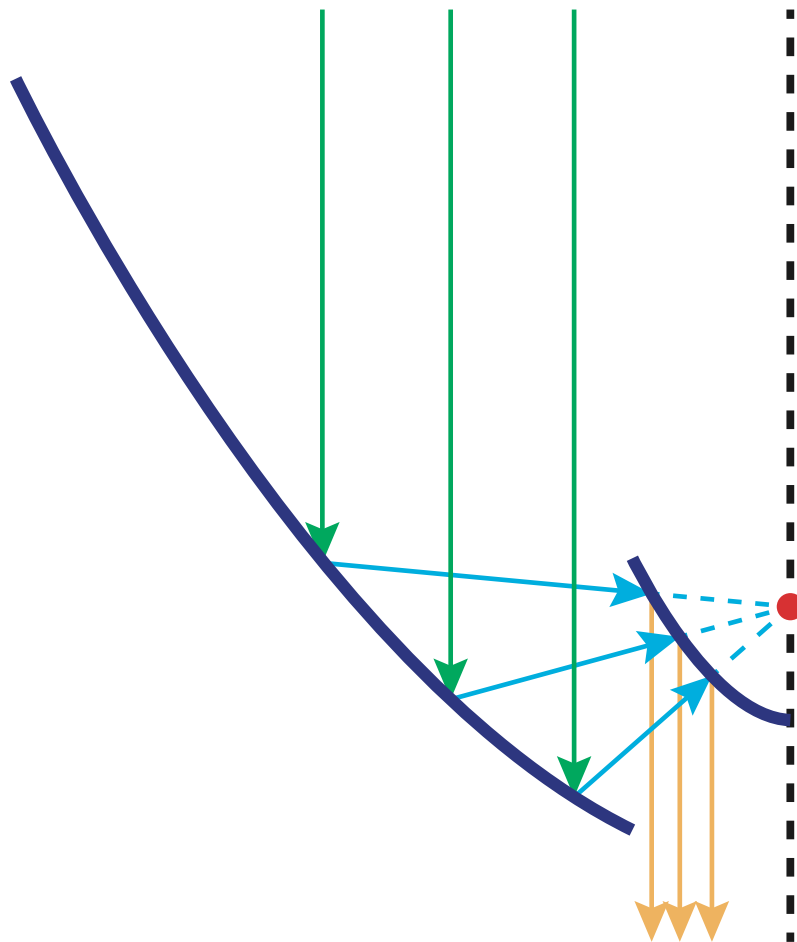
FIGURE 2.4 The structure composed of concave and convex parabolic mirrors. The concave mirror converts parallel light from above the system into focusing light. Focusing light by the concave mirror is converted into highly-dense parallel light by the convex mirror.

Figure 2.4 shows the structure composed of concave and convex parabolic structure (the CCCP system). This system can control light density and realise to convert parallel light into a highly-dense parallel. The most remarkable feature of the CCCP structure is that this structure does not have any focal points. We explain this feature's advantage when the structure is applied to daylighting systems, in the next chapter.

2.4 Zone Classification

The CCCP system can separate three types of conditions and four types of rays of light. We classify four types of rays into four zones.

Figure 2.5 shows the CCCP system and the expected rays. In Region (A), the first mirror reflects rays of light and the second mirror does not receive the rays. In Region (B), the first mirror reflects rays of light and generates focusing light. The second mirror reflects the rays into parallel. Here, the first mirror interrupts the path of the rays. Therefore, hereafter, we remove the interrupted region of the first mirror. In, Region (C), the wrong side of the first mirror absorbs light rays.
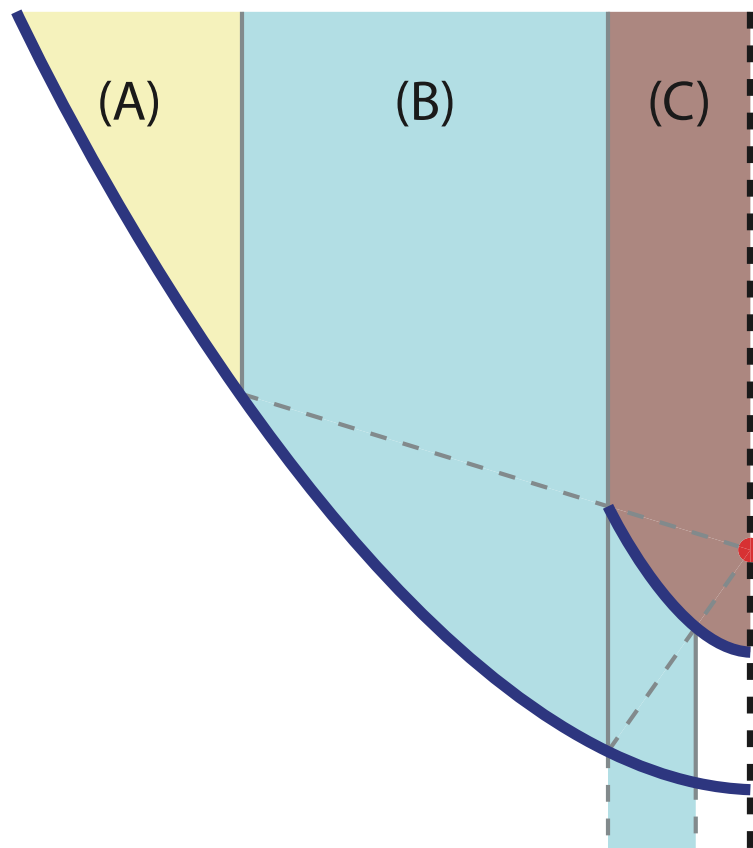
FIGURE 2.5 The CCCP system and the expected rays. There are three types of rays of light: Region (A), Region (B) and Region (C). Only rays in Region (B) realise to convert parallel light into a highly-dense parallel one.

Hereafter, we consider rotating the first mirror at a focal point.

2.5 Rotation

Here, we consider three types of conditions when the CCCP system rotates. As mentioned below, the no rotated case (basically case of Figure 2.5) includes slightly rotated case as the particular case.

Figure 2.6 shows three types of conditions of the CCCP system. The left panel shows the slightly rotated case. When the first mirror rotates slightly, there have three regions: Region (A), Region (B) and Region (C). In this case, it is entirely same as no rotated case shown as Figure 2.6.

The middle panel shows the rotated case. When the first mirror rotates, there have four regions: Region (A), Region (B), Region (C) and Region (X). Region (A)–(C) is the same as no rotated case. Region (X) shows no reflection and rays of light passing through between the first mirror and the second mirror. In this region, the amount of incoming rays (i.e. rays in Region (B)) decreases corre-

sponding to the rotation angle of the first mirror increases.

The right panel shows the excessively rotated case When the first mirror rotates excessively, there have three cases: Region (A), Region (C) and Region (X). In this case, there are no rays to convert parallel light into highly-dense parallel one (i.e. no rays in Region (B)). Besides, we need to mention one particular case. Region (X) is not always necessary. There is some particular case that the CCCP system does not have Region (X).

2.6   Summary

We summarise the main results of this chapter as below (points 1–2):

1.   We solved equation (2.6) and proved the feature of a parabolic mirror as equation (2.19) and Figure 2.2.

2.   The feature of a parabolic mirror can be comprehended easily and briefly using some well-known geometry and physics theories.

3.   We defined and explained a new-type structure, the CCCP structure.

4.   We classify incoming rays into four zones and investigate the case that the CCCP system rotates.

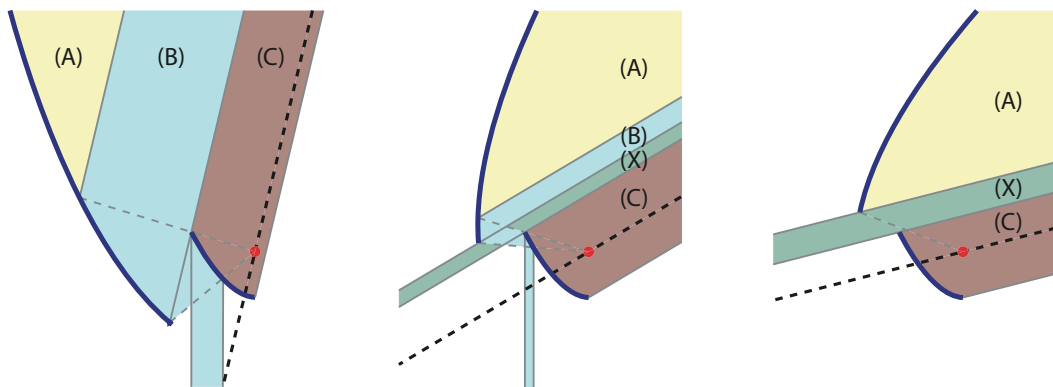In the next chapter, we estimate the performance of CCCP structure and discuss the results.

FIGURE 2.6 Three types of conditions of the CCCP system. The left panel is the slightly rotated case. The middle panel is the rotated case. The right panel is the excessively rotated case.

3 | METHODOLOGY

In this chapter, we set up the model of our new-type daylighting system, the CCCP daylighting system. First, we explain and show the basic structure of the system. Next, we define the model of the CCCP daylighting system geometrically. Finally, we perform test simulations of this system using two-dimensional ray-tracing codes and introduce performance indexes.

3.1 Basic Structure

At first, we explain the basic structure of the CCCP daylighting system. The CCCP daylighting system is composed of two paraboloids.
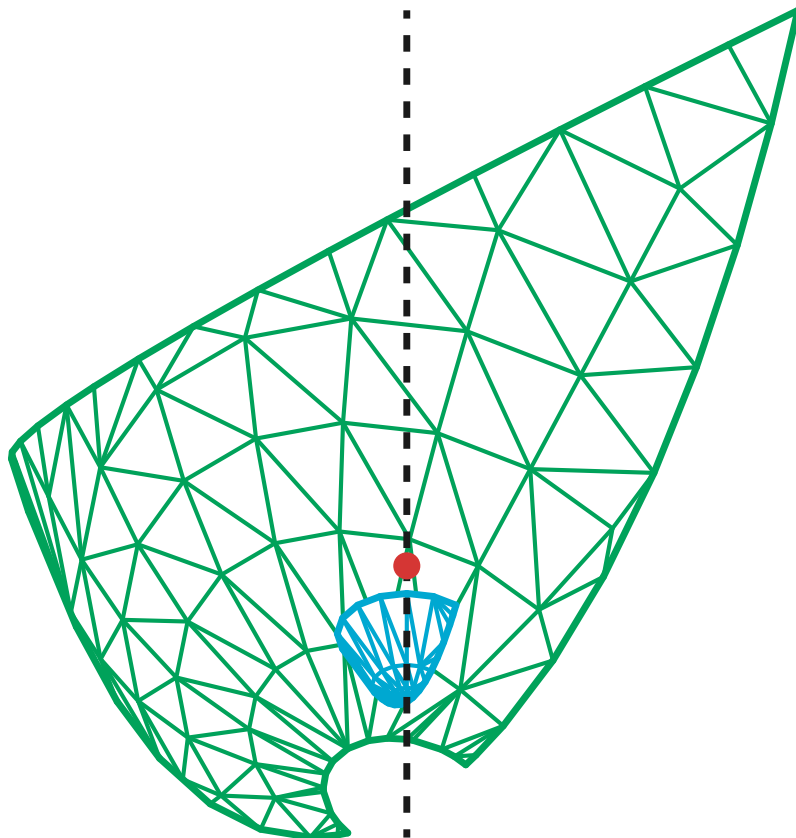
FIGURE 3.1 A new-type daylighting system, the CCCP daylighting system, composed of two paraboloids. The large concave paraboloidal mirror is the first mirror, and the small convex one is a second mirror. The first mirror moves and tracks the sun. The second one is fixed. This system has a two-freedom degree.

Figure 3.1 shows the basic structure of the CCCP daylighting system composed of two paraboloids with the same focal points. The system has a two-freedom degree: a vertical rotation of the first mirror and a horizontal rotation of the system. The first mirror collects sunlight and reflects the second mirror while focusing. The second mirror receives reflected light from the first mirror and reflects before passing through a focal point as focusing parallel light.

There are three points that the CCCP daylighting system has a significant advantage. First, there are no focal points. Second, the system does not create any spectrum. Last, it has two degrees of freedom. The CCCP daylighting system does not have any focal points, does not occur any spectrum, have enough less moving parts.

Similar work has been done by Ullah and Shin (2012, 2013), Ullah and Whang (2015). They use a similar system composed of concave and convex parabolic mirrors (Hereafter, Ullah system). However, there have two differences between Ullah system and the CCCP system. These two differences are also two great advantage of the CCCP system against Ullah system.

The first one is a degree of freedom. Ullah system has a three-freedom degree. In contrast, the CCCP system has a two-freedom degree. It means the CCCP system realises the same result as Ullah system with fewer moving parts. Ullah system has only two moving parts. In order to reduce a moving part, the system applied optical fibres.

The second advantage point is the centre of gravity. Ullah system needs to support two mirrors (i.e. one concave mirror and one convex mirror) from the convex mirror's bottom. It means the system needs a high moment of inertia, and the high load is applied to moving parts. In contrast, the CCCP system supports only the concave mirror and reduces the load. Besides, it is easy to increase in size when needed.

We adopt paraboloidal mirrors instead of parabolic column mirrors. Figure 3.2 shows the photorealistic three-dimensional computer graphics image of the CCCP daylighting system rendered by Arnold for Maya 3.1.2. The CCCP daylighting system has two types of paraboloidal mirrors: a concave mirror (Mirror I) and a convex mirror (Mirror II). The mirror I moves and tracks the sun. The Mirror II is fixed.

There is two advantage to use paraboloid. The first one is the compactness. The system needs to follow sunlight when used as daylighting systems. Paraboloidal systems need smaller space than parabolic column systems, in particular, at system width. The second advantage is density. Paraboloids increase density three-dimensionally and parabolic columns increase two-dimensionally. We adopt paraboloidal mirrors due to these advantages.

3.2 Geometric Definition

To realise our new-type daylighting system, CCCP daylighting system, we define the system's geometric feature mathematically.

Figure 3.3 shows a mathematical cross-section model of the CCCP daylighting system. We consider a three-dimensional model and the model consists of two paraboloidal mirrors that have the same rotation axis.

Our simulation model set-up considers the direct parallel sunlight. We set a function of the Mirror I $r_{\mathrm{I}}(t, \theta)$ and a function of the Mirror II $r_{\mathrm{II}}(t)$ to define

shapes of the mirrors analytically:

$$\boldsymbol{r}_{\mathrm{I}}(t,\theta) = A(\theta)\,\boldsymbol{r}_{\mathrm{I}}(t), \tag{3.1}$$

$$\boldsymbol{r}_{\mathrm{II}}(t) = \begin{pmatrix} t \\ \dfrac{1}{4\ell_{\mathrm{II}}}t^2 - \ell_{\mathrm{II}} \end{pmatrix}, \tag{3.2}$$

where

$$A(\theta) = \begin{pmatrix} \sin\theta & \cos\theta \\ -\cos\theta & \sin\theta \end{pmatrix}, \tag{3.3}$$

$$\boldsymbol{r}_{\mathrm{I}}(t) = \begin{pmatrix} t \\ \dfrac{1}{4\ell_{\mathrm{I}}}t^2 - \ell_{\mathrm{I}} \end{pmatrix}. \tag{3.4}$$

θ is the solar elevation, ℓ_I is a distance of the Mirror I's focal point, ℓ_{II} is a distance of the Mirror II's focal point.

Using equations (3.1)–(3.2), initial positions of mirrors (i.e. $\theta = 0$, see Fig-

ure 3.4) are determined analytically as

$$x_{I,L} = d_I, \tag{3.5}$$

$$x_{I,R} = -2\ell_I \tan\theta_{max} \left(1 - \sqrt{1 + \frac{1}{\tan^2\theta_{max}} \left(1 + \frac{x_{II,L}}{\ell_I \cos\theta_{max}} \right)} \right), \tag{3.6}$$

$$x_{II,L} = 2\ell_{II} \left(a(x_{I,L}, \theta_{max}) - \sqrt{a^2(x_{I,L}, \theta_{max}) + 1} \right), \tag{3.7}$$

$$x_{II,R} = 2\ell_{II} \left(a(X, \theta_{max}) - \sqrt{a^2(X, \theta_{max}) + 1} \right), \tag{3.8}$$

where

$$a(t, \theta) = \frac{r_{I,y}(t, \theta)}{r_{I,x}(t, \theta)}, \tag{3.9}$$

$$X = -Y \cos\theta_{max}, \tag{3.10}$$

$$Y = r_{II,y}(x_{II,L}, \theta_{max}) - x_{II,L} \tan\theta_{max}. \tag{3.11}$$

Here, $x_{I,L}$ is a left-end of the Mirror I, $x_{I,R}$ is a right-end of the Mirror I, $x_{II,L}$ is a left-end of the Mirror II, $x_{II,R}$ is a right-end of the Mirror II, d_I is initial condition of $x_{I,L}$ and θ_{max} is the culmination altitude in the summer solitude:

$$\theta_{max} = 90 - \lambda + 23.45. \tag{3.12}$$

Here, λ is the latitude in a degree. Equations (3.5)–(3.8) define a shape of our

daylighting system with four initial conditions: λ, ℓ_{I}, ℓ_{II} and d_{I}.

3.3 Test Simulation

First, we perform several test simulations. In this paper, we use the two-dimensional ray-tracing algorithm as simulation codes.

3.3.1 Ray Tracing Algorithm

Ray tracing is one of the well-known algorithms in graphics to trace the path of rays. We adopt the forward recursive ray tracing algorithm to trace and detect the rays conducted inside the CCCP system. Forward ray tracing traces rays from light sources.

In our simulations, we set up only direct sunlight as a light source and do not consider diffuse reflection because the interest of this paper is how to control light flow and density. To estimate some physical states, we set two physical constants: the solar illuminance constant $E_{\odot} = 1.34 \times 10^5$ lx and atmospheric

transmissivity $\tau_\odot = 0.65$.

3.3.2 Initial Condition

TABLE 3.1 Simulations of resolution dependence.

Run	λ	N	ℓ_{I}	ℓ_{II}	d_{I}
ID	[deg]	[-/m]	[m]	[m]	[m]
1	30	1	4.0	1.0	8.0
2	30	5	4.0	1.0	8.0
3	30	10	4.0	1.0	8.0
4	30	20	4.0	1.0	8.0

A series of simulations are resolution dependence (i.e. a number of rays in ray-tracing simulations) as listed Table 3.1. Here, the resolution N means line density of rays in ray-tracing simulations. The purpose of these simulations is to check relationships between results and resolutions.

3.3.3 Daily Behaviour

Figure 3.5 shows ray-tracing images of Run 1 at summer solitude, 6.00 in top-left, 8.00 in top-right, 10.00 in bottom-left and 12.00 in bottom-right panels. The green-ray is an effective ray that is taken into the daylighting system by the collector. The red one is an ineffective ray that means out of the system. Figure 3.5 shows the CCCP daylighting system behaves that we expected.

On 21st June (i.e. at summer solitude), at 6.00, the daylighting system cannot get any effective rays for the solar elevation is too low elevation. At 8.00, several rays begin to enter inside the system. At 10.00, round half coming-to-Mirror-I rays are taken into the daylighting system. Moreover, at 12.00, culmination, the daylighting system acts the most effective in a year.

After 12.00, the system behaves inverse way. Behaviour at 14.00 is the same as at 10.00, behaviour at 16.00 is the same as at 8.00 and behaviour at 18.00 is the same as at 6.00. The system has line symmetry at culmination time. We can check this behaviour later.

3.3.4 Annual Behaviour

The one-year simulation is one of the most influential and convenient figures to know the performance of daylighting systems (cf. (Mardaljevic 2000)).

Figure 3.6 shows the one-year simulations of resolution dependence to Run 1–4, Run 1 ($N = 1$) in top-left, Run 2 ($N = 5$) in top-right, Run 3 ($N = 10$) in bottom-left and Run 4 ($N = 20$) in bottom-right panels, with illuminance rate. The illuminance rate r_E is defined as

$$r_E = \frac{\bar{E}_{\text{out}}}{\bar{E}_{\text{in}}}. \tag{3.13}$$

Here, $\bar{E}_{\text{out}}$ is the mean illuminance taken into our daylighting system (i.e. the illuminance at the yellow line, which shows end of the collector). $\bar{E}_{\text{in}}$ is the mean illuminance struck the Mirror I.

Figure 3.6 illustrates concentric distributions of illuminance rate. One year simulations provide an understandable figure to estimate the performance of daylighting systems.

First, Run 1 (i.e. $N = 1$) does not have enough resolutions to express the illuminance rate. From Run 1 to Run 4, the distributions get smoother and smoother as the resolutions are higher and higher. For our simulations, Run 4, $N = 20$, seems enough high resolutions.

Besides, we refer to the calculation time. In general, in ray-tracing simulations, the calculation time becomes higher following its resolutions. Therefore, we adopt Run 4 as a standard of resolutions (i.e. $N = 20$) because Run 4 has enough resolution in our simulations. Hereafter, we use $N = 20$ for every simulations.

The one-year simulation of Run 4 (on bottom-right panels in Figure 3.6) shows features of the CCCP daylighting system. The centre of concentric circles is summer solitude. At 12.00 of summer solitude, the illuminance rate reaches the maximum value. And the illuminance rate decrease in concentric circles from the centre.

3.4 Performance Index

According to the result of Run 4, we can get three features as below (point 1–3):

1. At summer solitude, at 12.00, the illuminance rate is maximum.

2. At summer solitude, the adequate time, which means the CCCP daylighting system acts effectively throughout the day (i.e. the illuminance rate is more than 1.0), is also maximum.

3. At winter solitude, the effect is minimal.

According to these features, we have three strategies to approach more effective results as below (point 4–6):

4. To maximise the effective time at summer solitude.

5. To maximise the effective time at winter solitude.

6. To maximise the annual lighting efficiency, which means how long daylighting systems are available in a year.

It seems better to maximise the illuminance rate at summer solitude, at 12.00. However, we do not accept this strategy because, in general, it is not so important to maximise the illuminance rate at some point. It is essential to maximise the effective time or the mean illuminance rate. In our model, the illuminance rate has many ups and downs. The illuminance rate varies enormously, especially at round 12.00.

Therefore, the mean illuminance rate is not convenient at least to the CCCP daylighting system. So we check three values corresponding the three strategies, the maximum effective time T_{max}, the minimum effective time T_{min} and the an-

nual lighting efficiency p_{yr}:

$$T_{max} = \int_{r_E > 1 \wedge S_S} dt, \tag{3.14}$$

$$T_{min} = \int_{r_E > 1 \wedge S_W} dt, \tag{3.15}$$

$$p_{yr} = \frac{\int_{r_E > 1 \wedge U} dt}{\int_U dt}, \tag{3.16}$$

where S_S is a set of a time in summer solitude, S_W is a set of a time in winter solitude and U is a set of a time in a year.

Figure 3.7 shows the performance of daylighting systems from equations (3.14)–(3.16). In this occasion, Our system could be used throughout the year. Basically, in summer, the system works at most 8.5 hours. In winter, it works at least 3.75 hours. Moreover, our system could be used 26.8% throughout the year. This our new-type estimation of the performance of daylighting systems is instrumental in comparing the performance of systems.

3.5 Summary

We summarise the main results of this chapter as below (point 1–3):

1.   We set-up the geometric model of the CCCP daylighting system mathematically.

2.   We test the behaviour of the CCCP daylighting system.

3.   To estimate the performance of daylighting systems, we define three performance indexes.

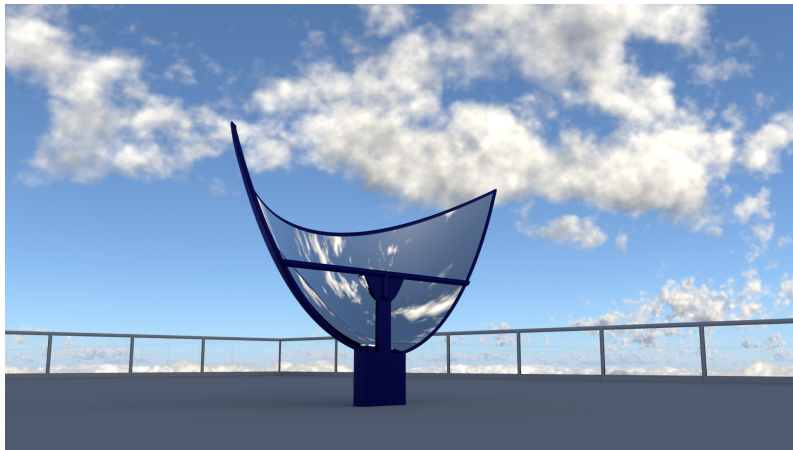Next chapter, we discuss shape dependence of the CCCP daylighting system.

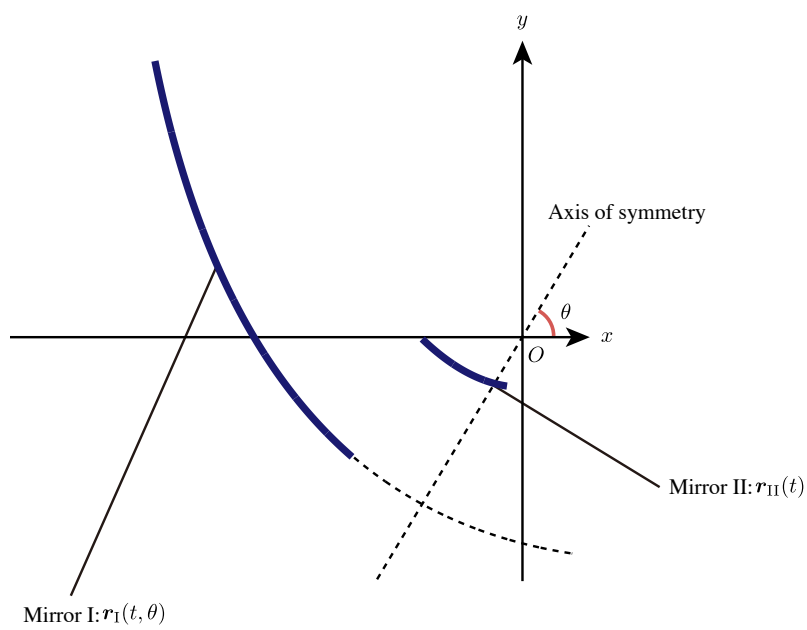**FIGURE 3.2** Photorealistic image of the CCCP daylighting system.

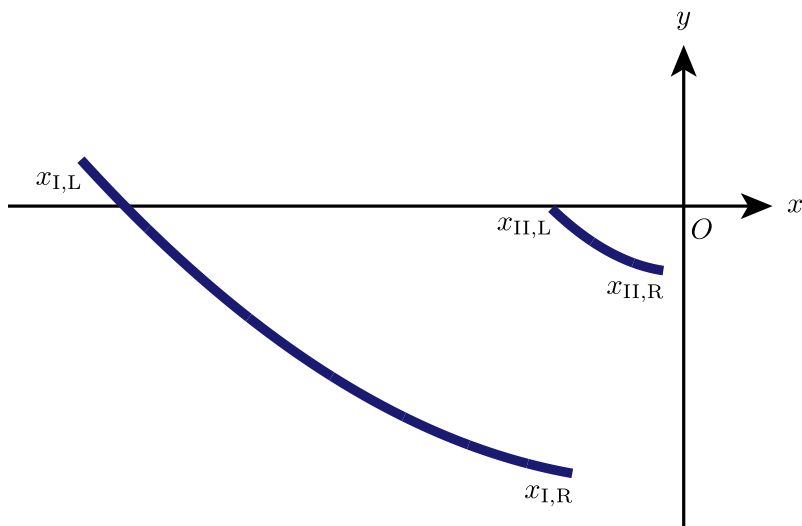**FIGURE 3.3** Mathematical cross-section model of our daylighting system.

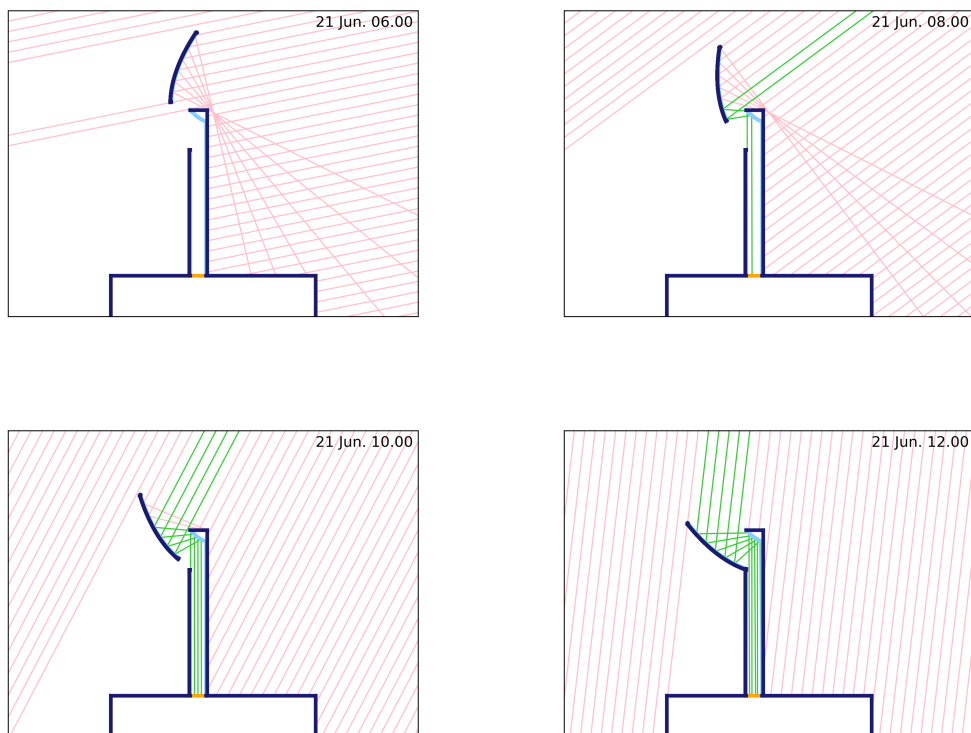**FIGURE 3.4** Initial positions of mirrors.

FIGURE 3.5 Ray-tracing images of Run 1 at summer solitude. 6.00 is in the top-left panel, 8.00 is in the top-right panel, 10.00 is in the bottom-left panel, and 12.00 is in the bottom-right panel.
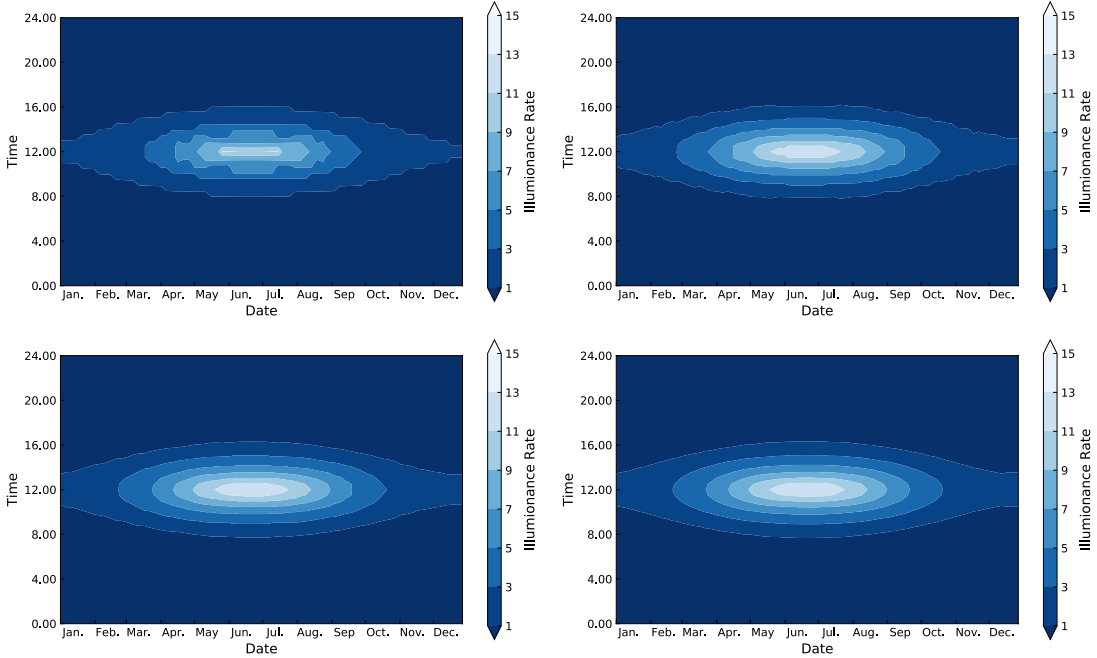
FIGURE 3.6 The One-year simulation of resolution dependence to Run 1–4. Run 1 is in the top-left panel, Run 2 is in the top-right panel, Run 3 is in the bottom-left panel and Run 4 is in the bottom-right panel.
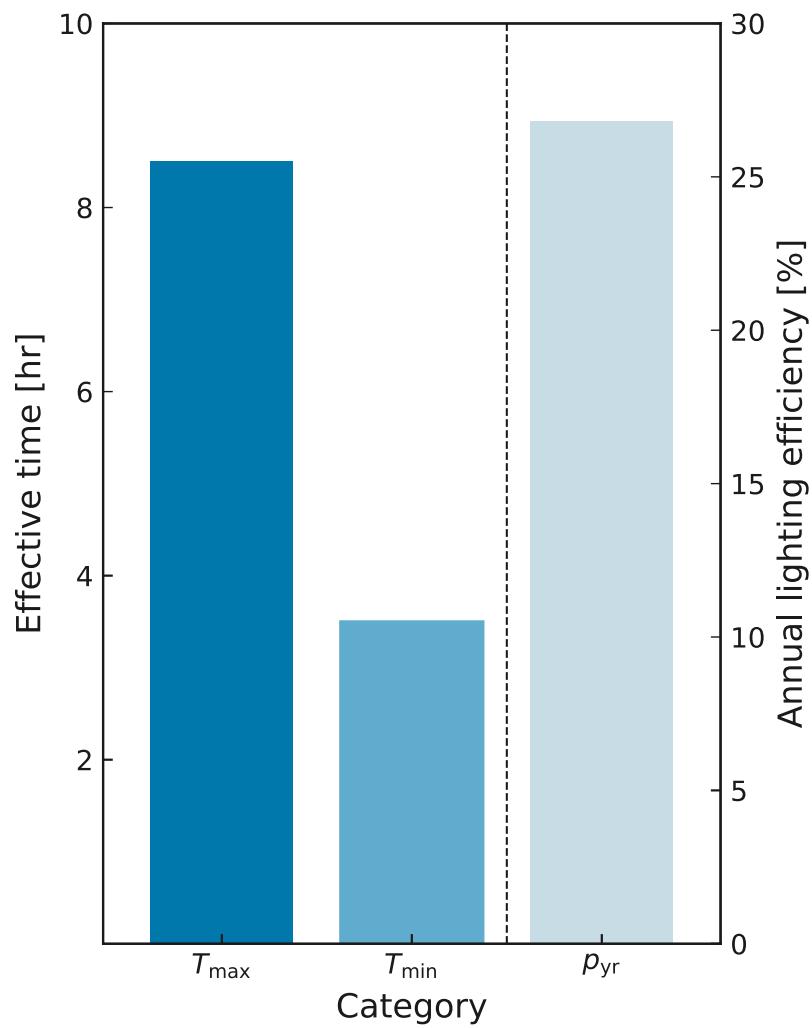
FIGURE 3.7 The performance of daylighting systems by three strategies. Three of these parameters shows the performance of the systems.

4 | SHAPE DEPENDENCE

In this chapter, we discuss the results of shape dependence. There are three dependence to shapes: the distance between the Mirror I and the focal point, the Mirror II and the focal point, and the sizer of the Mirror I (the size of the Mirror II are determined when the size of Mirror I is determined). The last of this chapter, we get the CCCP daylighting system's optimised shape as the shape dependence.

4.1   Mirror I Distance Dependence

First of all, we perform a series of simulations of the Mirror I distance dependence (i.e. the distance between the Mirror I and the focal point) as listed in Table 4.1. In this section, we compare Run 4 ($\ell_I = 4.0$), Run 5 ($\ell_I = 2.0$), Run 6 ($\ell_I = 6.0$)

and Run 7 ($\ell_I = 8.0$).

Figure 4.1 shows the one-year simulations of the Mirror I distance depen-
dence to Run 5–7, Run 4 ($\ell_I = 4.0$) in top-left as a standard of simulations, Run 5
($\ell_I = 2.0$) in top-right, Run 6 ($\ell_I = 6.0$) in bottom-left and Run 7 ($\ell_I = 8.0$) in
bottom-right panels, with illuminance rate. The figure illustrates the feature and
performance of our daylighting systems. According to our strategies (see Chap-
ter 3), Run 4 or Run 6 seems to have good performance. Like this, the one-year
simulation is convenient to check the performance briefly and visually.

However, when we want to know the detailed performance of daylighting
systems, the one-year simulation is not suitable. In this occasion (i.e. Run 4 vs
Run 6), it is not easy to choose which result is the best. Then, we consider the
performance indexes that we defined in Chapter 3; the maximum effective time
T_{max}, the minimum effective time T_{min} and the annual lighting efficiency p_{yr}, to
check the detailed performances.

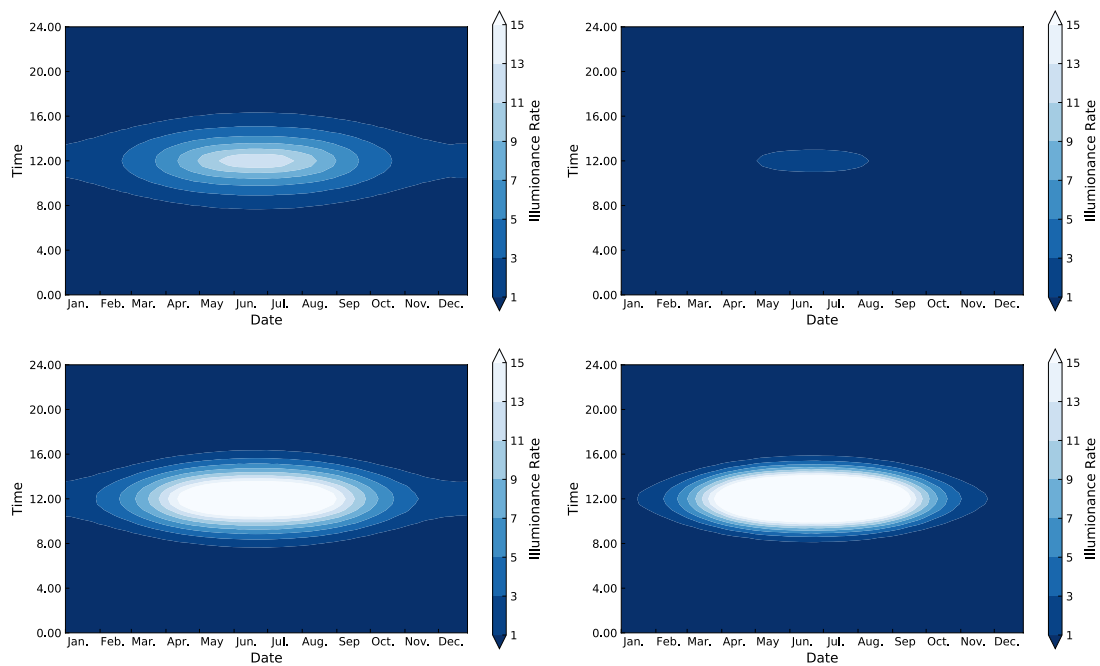Figure 4.2 shows the performance indexes; the maximum effective time in

FIGURE 4.1 The one-year simulations of the Mirror I distance dependence to Run 4 and Run 5–7. Run 4 is in the top-left panel as a standard of simulations, Run 5 is in the top-right panel, Run 6 is in the bottom-left panel and Run 7 is in the bottom-right panel.
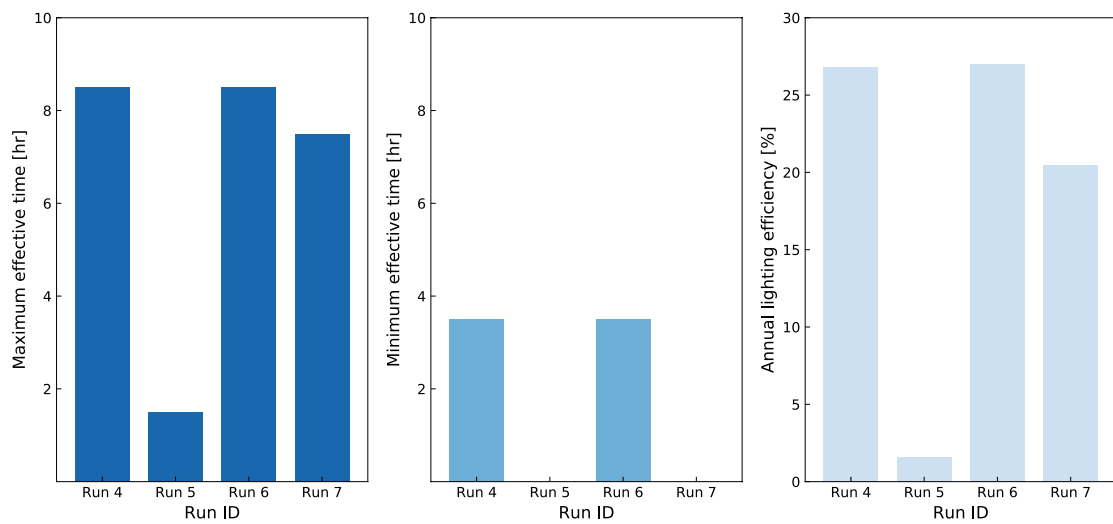
FIGURE 4.2 The performance indexes to Run 4 and Run 5–7. The maximum effective time is in the left panel, the minimum effective time is in the middle panel, and the annual lighting efficiency is in the right panel.

left, the minimum effective time in middle and the annual lighting efficiency in the right. The left figure illustrates that Run 4 and Run 6 have good performance at the summer solstice. The middle figure illustrates that Run 5 and Run 7 are entirely useless in the winter solstice. These two results show that Run 4 or Run 6 has good performance as a result of optimisation.

Moreover, we should decide which Run gives us good performance Run 4 or Run 6. The answer is in the right figure, the annual lighting efficiency. The figure illustrates that Run 6 has better performance than Run 6. Therefore Run 6 is the best answer in all Runs.

Then, we perform an additional simulation as listed in Table 4.2. Here, the difference between Run 6 and Run 8 is the value of ℓ_I. Run 6 is $\ell_I = 6.0$ and Run 8 is $\ell_I = 5.0$. Run 8 means the intermediate state between Run 4 and Run 6. This simulation is performed to find the extremum of the performance between $\ell_I = 4.0$ and $\ell_I = 6.0$.

Figure 4.3 shows an additional simulations to Run 8, Run 6 ($\ell_I = 6.0$) is left

TABLE 4.1 Simulations of Mirror I distance dependence.

Run ID	λ [deg]	N [-/m]	ℓ_{I} [m]	ℓ_{II} [m]	d_{I} [m]
4	30	20	4.0	1.0	8.0
5	30	20	2.0	1.0	8.0
6	30	20	6.0	1.0	8.0
7	30	20	8.0	1.0	8.0

TABLE 4.2 Additional simulation of Mirror I distance dependence.

Run ID	λ [deg]	N [-/m]	ℓ_{I} [m]	ℓ_{II} [m]	d_{I} [m]
6	30	20	6.0	1.0	8.0
8	30	20	5.0	2.0	8.0

as a standard of simulations and Run 8 ($\ell_I = 5.0$) in right panels, with illuminance rate. This figure illustrates that Run 6 is better than Run 8 for the value of the maximum illuminance rate. However, now, we are interested in three values because of the one-year performance. Therefore we compare three values.

Figure 4.4 shows the performance indexes; the maximum effective time in left, the minimum effective time in middle and the annual lighting efficiency in the right. The left figure and the middle figure do not give us enough information about that because there is not any difference between the two of them. However, the right figure gives essential information.

Following Figure 4.3, Run 6 looks better than Run 8 as the maximum, and the total illuminance rate looks higher than Run 8. Figure **??**, the right panel shows that Run 8 is ultimately better than Run 6 because of the annual lighting efficiency. According to our strategies, it is essential to maximise the annual lighting efficiency to make an efficient daylighting system. Therefore, in this case, we conclude that Run 8 is better than Run 6, and we adopt Run 8 as the standard of simulations.

4.2 Mirror II Distance Dependence

TABLE 4.3 Simulations of the Mirror II distance dependence.

Run ID	λ [deg]	N [-/m]	ℓ_{I} [m]	ℓ_{II} [m]	d_{I} [m]
8	30	20	5.0	1.0	8.0
9	30	20	2.0	2.0	8.0
10	30	20	6.0	3.0	8.0
11	30	20	8.0	4.0	8.0

Second, we perform a series of simulations of the Mirror II distance dependence (i.e. the distance between the Mirror II and the focal point) as listed Table 4.3. In this section, we compare Run 8 ($\ell_{\mathrm{II}} = 1.0$), Run 9 ($\ell_{\mathrm{II}} = 2.0$), Run 10 ($\ell_{\mathrm{II}} = 3.0$) and Run 11 ($\ell_{\mathrm{II}} = 4.0$).

Figure 4.5 shows one-year simulations of the Mirror II distance dependence to Run 9–11, Run 8 ($\ell_{\mathrm{II}} = 1.0$) in top-left as a standard of simulations, Run 9 ($\ell_{\mathrm{II}} = 2.0$) in top-right, Run 10 ($\ell_{\mathrm{II}} = 3.0$) in bottom-left and Run 11 ($\ell_{\mathrm{I}} = 4.0$) in bottom-right panels, with the illuminance rate.

The figure illustrates that Run 8 is the best result in this section. Therefore, we do not need to consider the performance indexes; the maximum effective time, the minimum effective time and the annual lighting efficiency. Run 8 is the best in this section from the one-year simulations. Moreover, we also conclude that the one-year simulations are useful and straightforward to check the apparent results.

4.3 Mirror I Size Dependence

TABLE 4.4 Simulations of the Mirror I size dependence.

Run ID	λ [deg]	N [-/m]	ℓ_{I} [m]	ℓ_{II} [m]	d_{I} [m]
8	30	20	5.0	1.0	8.0
12	30	20	5.0	1.0	2.0
13	30	20	5.0	1.0	4.0
14	30	20	5.0	1.0	6.0

Finally, we perform a series of simulations of the Mirror I size dependence (i.e. a left edge of Mirror I) as listed Table 4.3. In this section, we compare Run 8

($d_I = 8.0$), Run 12 ($d_I = 2.0$), Run 13 ($d_I = 4.0$) and Run 14 ($d_I = 6.0$).

Figure 4.6 shows one-year simulations of the Mirror II size dependence to Run 12–14, Run 8 ($d_I = 8.0$) in top-left as a standard of simulations, Run 12 ($d_I = 2.0$) in top-right, Run 13 ($d_I = 4.0$) in bottom-left and Run 14 ($d_I = 6.0$) in bottom-right panels, with illuminance rate.The figure illustrates Run 8 or Run 14 have better performance in this section.

However, following our strategies, Run 12 is not a relevant result because it has no illuminance rate in the winter solstice. We demand that the CCCP daylighting system is available throughout the year. Figure **??** obviously gives this information completely easy. Therefore, here, we do not consider the performance indexes. Run 8 is the best in this section from the one-year simulations. Finally, we can get Run 8 has the best performance in our simulation ranges as the optimised result.

4.4 Summary

We summarise The main results of this chapter as below (point 1–3):

1. We check the Mirror I distance dependence using the results of the one-year simulations and the performance indexes.

2. We perform a series of simulations of the Mirror II distance dependence and the Mirror I size dependence with the Mirror I distance dependence.

3. Form these simulations, we get the result of Run 8 ($\ell_{\mathrm{I}} = 5.0$, $\ell_{\mathrm{II}} = 1.0$, $d_{\mathrm{I}} = 8.0$) as the optimised shape of the CCCP daylighting system.

Next chapter, we discuss geographic dependence (i.e. the latitude dependence) of the CCCP daylighting system using the optimised shape derived from this chapter's result.
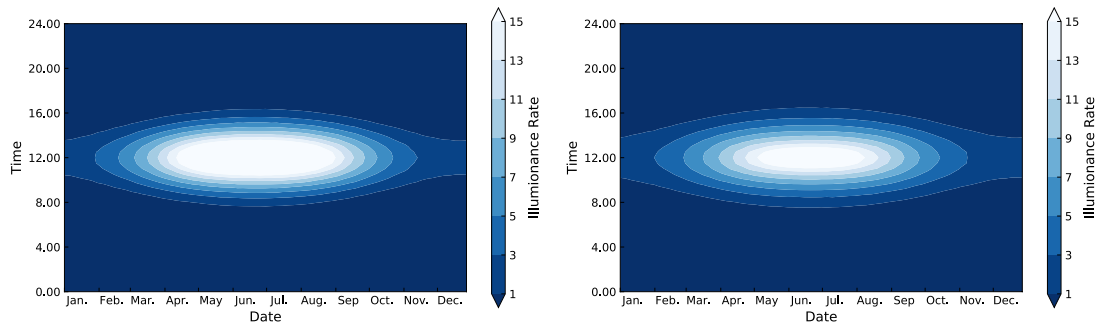
FIGURE 4.3 The one-year simulations of an additional simulation to Run 6 and Run 8. Run 6 is in the left panel as a standard of simulations, and Run 8 is in the right panel.
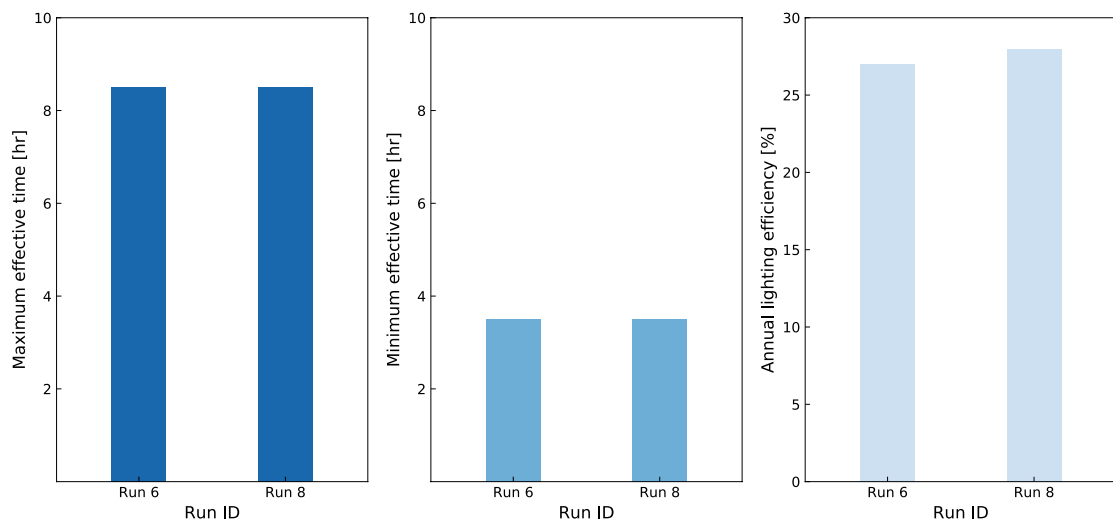
FIGURE 4.4 The performance indexes to Run 6 and Run 8. The maximum effective time is in the left panel, the minimum effective time is in the middle panel, and the annual lighting efficiency is in the right panel.
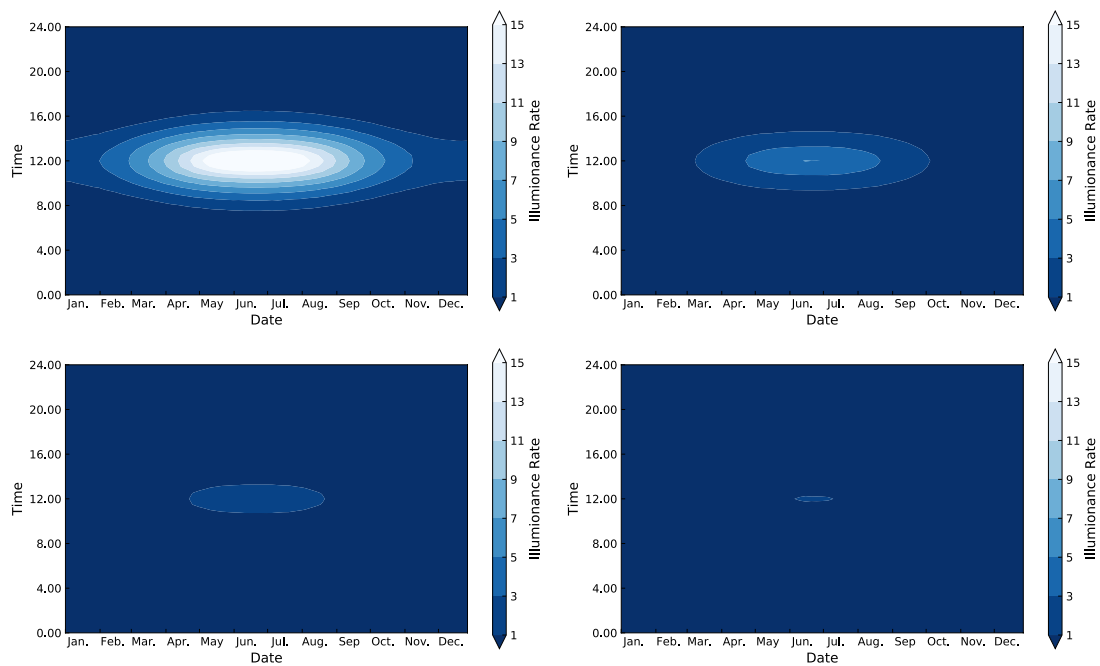
FIGURE 4.5 The one-year simulations of Mirror II distance dependence to Run 8 and Run 9–11. Run 8 is in the top-left panel as a standard of simulations, Run 9 is in the top-right panel, Run 10 is in the bottom-left panel and Run 11 is in the bottom-right panel.
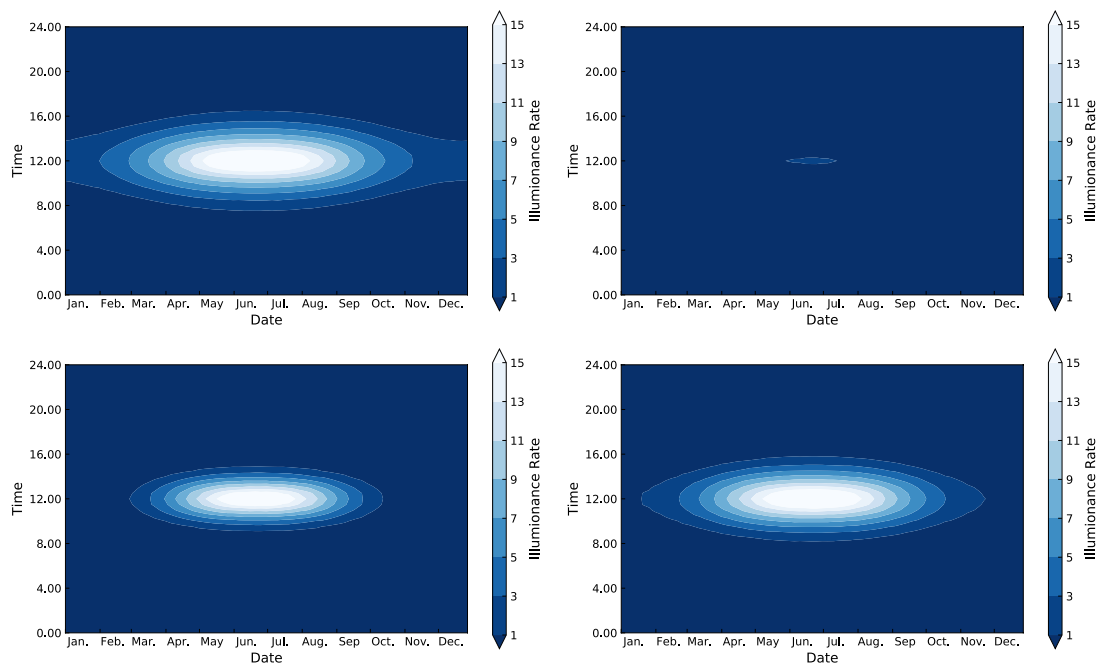
FIGURE 4.6 The one-year simulations of the Mirror II size dependence to Run 8 and Run 12–14. Run 8 is in the top-left panel as a standard of simulations, Run 12 is in the top-right panel, Run 13 is in the bottom-left panel and Run 14 is in the bottom-right panel.

5 | GEOGRAPHIC DEPENDANCE

In this chapter, we discuss the results of shape dependence. There are three dependence to shapes: the distance between the Mirror I and the focal point, the Mirror II and the focal point, and the sizer of the Mirror I (the size of the Mirror II are determined when the size of Mirror I is determined). The last of this chapter, we get the CCCP daylighting system's optimised shape as the shape dependence.

5.1 Latitude Dependence: at Specific Latitude

We perform a series of simulations of the latitude dependence at specific latitudes. These simulations are at several specific latitudes (i.e. from $0°$ to $90°$, for every $5°$). Moreover, simulations use the optimised values in the previous chap-

ter (i.e. Run 8).

Figure 5.1 shows the simulations of the latitude dependence at specific latitude e from $0°$ to $30°$. From $0°$ to $20°$, there are two highest points of illuminance rate in the figures. At first glance, they look wrong results. However, they are completely correct. These phenomena are occurred by the axial tilt of the Earth.

The axial tilt of the Earth causes an interesting result. The highest solar elevation $90°$ at summer solstice is worked out at $23.45°$. $23.45°$ is the angle of the axial tilt of the Earth. After this latitude (i.e from $0°$ to $23.45°$), the solar elevations decrease from $23.45°$ at summer solstice. One of the important points of this argument is 'at summer solstice'.

The highest illuminance rate point is changed and moved from the summer solstice. Moreover, it divides two points at $23.45°$. This phenomenon is well-known in physics. However, many people do not know this real phenomenon. Because the ones living between the tropics only know this phenomenon in a real environment. One of the best points of this division is that the range of high
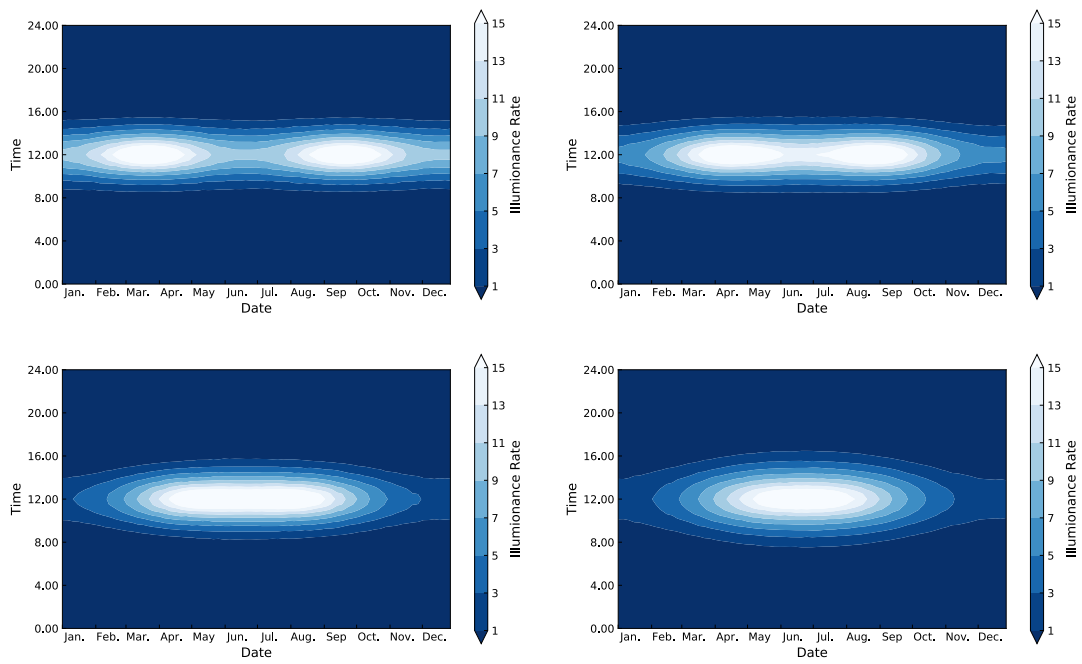
FIGURE 5.1 The latitude dependence at specific latitude from $0°$ to $30°$.

illuminance rate zone increases. Especially, we can get high illuminance rate in winter.

From 30° to 90°, the highest illuminance rate point is at summer solstice. Moreover, when the latitude increases, the effective time is spreading. At winter, the time is decreasing. Here, 'The effective time' is when daylighting systems can use effectively (i.e. the illuminance rate is greater than 1.0). At 90°, this figure shows that the CCCP daylighting system can not use at such latitude. Especially, from 50°, the system does not use effectively. This result is one of the improvable points of the CCCP daylighting system and should be improved.

5.2   Latitude Dependence: at Noon

Next, we perform a series of simulations of the latitude dependences at noon. These simulations are at several specific latitudes (i.e. from 0° to 90°, for every 5°). Moreover, simulations use the optimised shape derived in the previous chapter (i.e. Run 8).
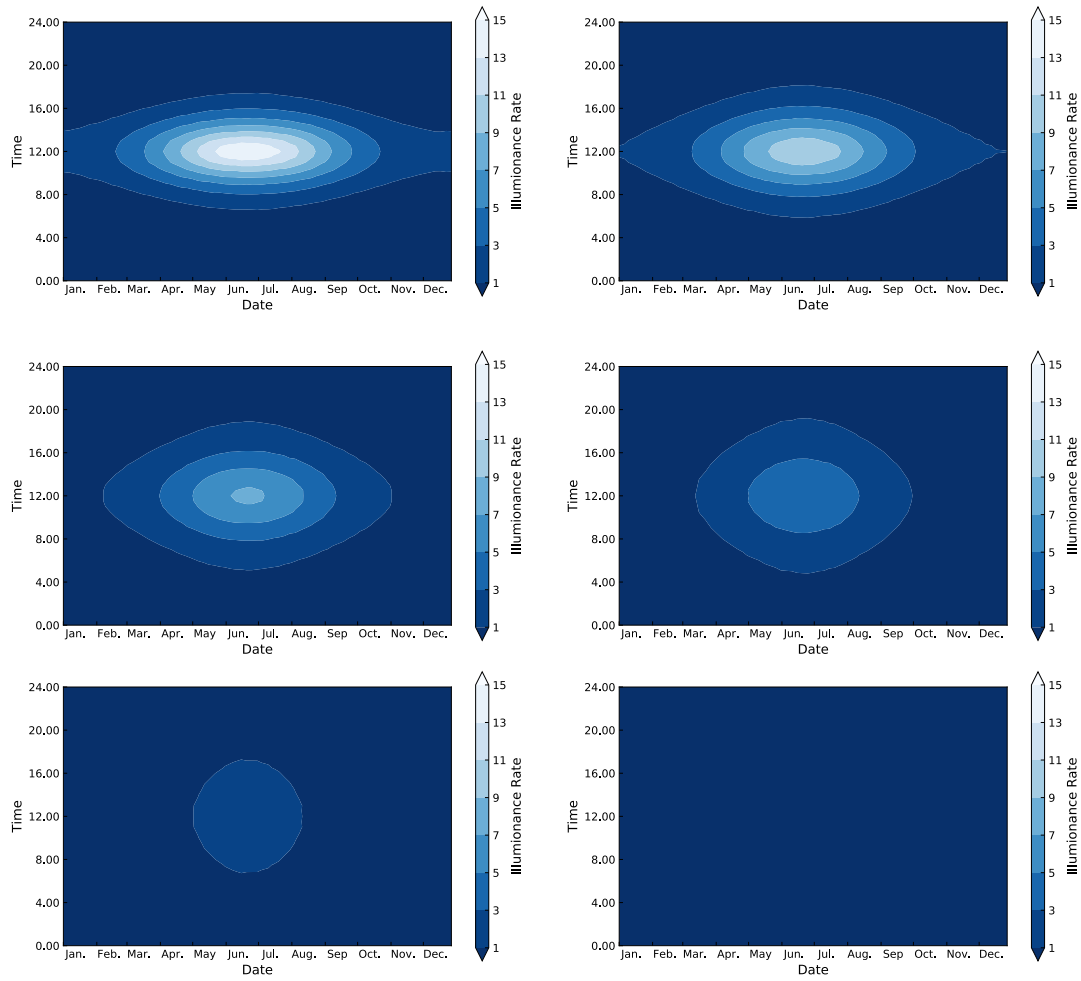
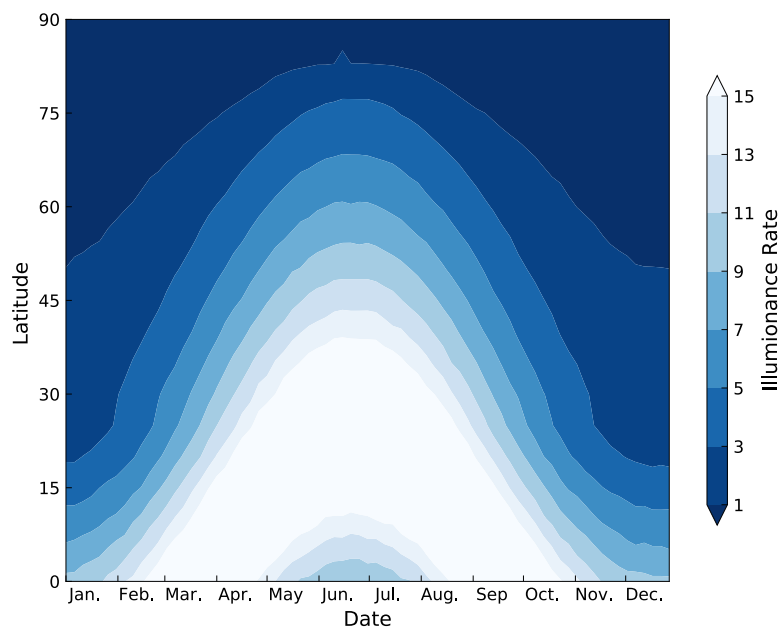**FIGURE 5.2** Latitude dependence at specific latitude from 40° to 90°.

FIGURE 5.3 Latitude dependences at noon.

Figure 5.3 shows the simulations of the latitude dependences at noon. The Y-axis shows latitudes. This figure suggests two crucial points to consider the latitude dependence of the CCCP daylighting system.

First one is that there are two highest illuminance rate points at the specific latitude. We have already mentioned this phenomenon in the previous section. The phenomenon is occurred by the axial tilt of the Earth. Moreover, this figure gives the zone of the highest illuminance (white coloured zone).

The second is that this figure shows the zone that we can use the CCCP daylighting system virtually. In this case, the maximum latitude that the CCCP daylighting system works effectively is under round $50°$. Over round $50°$, the system can not receive enough sunlight. When the latitude is over round $50°$, the illuminance rate becomes less than 1.0 at specific seasons (for instance, especially around winter solstice).

Figure 5.3 illustrates the illuminance rate 'at noon' for all seasons. Basically, at a certain latitude, when the illuminance rate is less than 1.0 at noon, the CCCP

daylighting system does not work for every season. It means the CCCP day-lighting system is completely useless at such a latitude. This result is one of the important points that we should improve.

We have also confirmed these points in the previous section. Using the latitude dependence at noon, we can check the threshold altitude quickly and briefly. However, it is not easy to know the one-year performance at a specific latitude. Therefore, both figure has each advantage.

5.3 Latitude Dependence: at Specific Seasons

The last, we perform a series of simulations of the latitude dependences at specific seasons. In this section, we choose two points as specific seasons: summer solstice and winter solstice. These simulations are at several specific latitudes (i.e. from $0°$ to $90°$, for every $5°$). Moreover, simulations use the optimised shape in the previous section (i.e. Run 8).

Figure 5.4 shows the simulations of the latitude dependences at summer

and winter solstice. The Y-axis shows latitudes. This figure gives us two important points.

First, at the summer solstice, the CCCP daylighting system can use for every latitude under $65°$ in the work-ng time. We define that the working time is from 8.00 through 16.00. We use the working time because we assume that the system is mainly used in the office.

Moreover, the reason that we put latitude threshold, under $65°$, is that all major city in the world is wholly located under $65°$. Therefore there is no meaning to consider the latitude over $65°$ in our study. In this assumption, we use the CCCP daylighting system effectively.

The second, in the winter solstice, the CCCP daylighting system never use virtually over round $50°$. In the first discussion, at the summer solstice, we mentioned that the CCCP daylighting system needs to be available under $65°$ due to the major city in the world is under $65°$. This result suggests that the optimised shape (i.e. Run 8) is not suitable. We should consider how to improve more

deeply.

5.4 Summary

We summarise the main results of this chapter as below (points 1–3):

1. The optimised CCCP daylighting system in the previous chapter (i.e. Run 8) works suitable under the latitude of 50°.

2. Under 23.45°, due to the axial tilt of the Earth, the CCCP daylighting system has two points of the highest illuminance rate.

3. We deeply consider to improve the system that works under 65°.

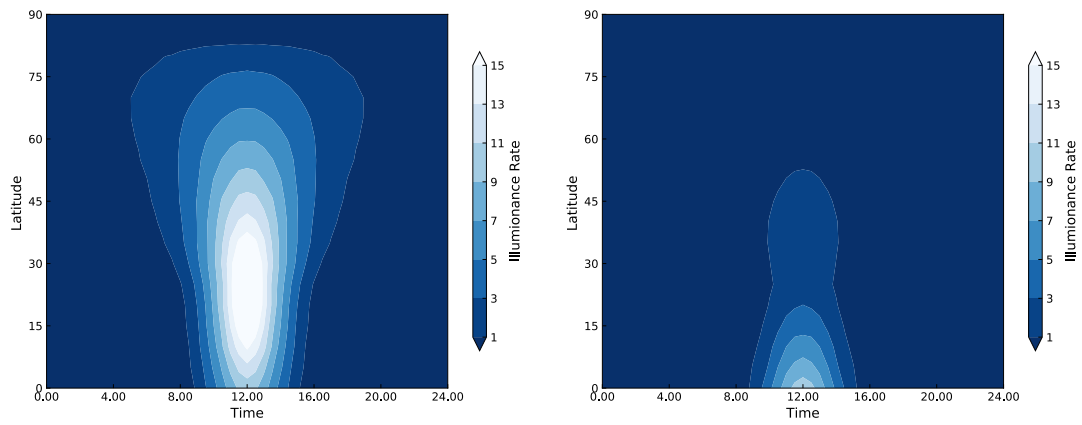In the next chapter, we surmise and conclude this thesis and discuss future work.

FIGURE 5.4 Latitude dependences at summer and winter solstice.

6 | CONCLUSION

In this chapter, we conclude this PhD thesis. We surmise each chapter's discussion, point out the issues that the CCCP daylighting system have and express the future work.

6.1 Summary

We summarise this PhD thesis in this section. First of all, this thesis's primary purpose is to propose the new-type non-focal direct sunlight daylighting system. We propose the innovative structure that does not have any focal points and realise to convert parallel light into a highly-dense parallel through the thesis. Moreover, we call this new-type structure composed of concave and convex

parabolic system (CCCP system).

In Chapter 1, first, we explain the background of the reason that the day-lighting systems are needed. Second, we give a detailed overview of daylighting systems and define the essential element to determine daylighting systems' performance, collectors. The last, we motivate the study of our new-type daylighting system, the CCCP daylighting system, and explain this PhD thesis's structure.

In Chapter 2, we introduce the essential and fundamental theory of this study, the CCCP structure. The basic theory of this chapter is the review of Tsuji and Suzuki (2017, 2019). First, we derive the essential feature of a parabolic mirror with the analytical method. Second, we consider the geometric feature of a parabolic mirror and define the CCCP structure. Finally, we discuss the CCCP structure's detailed feature to classify four types of rays into four zones.

In Chapter 3, we explain the methodology of our study. First, we introduce the CCCP daylighting system, compare our system and similar work (Ullah and Shin 2012, 2013, Ullah and Whang 2015) and indicate the advantage of the CCCP

daylighting system against the Ullah system. Second, we set up the model of the system and define the geometric feature of it mathematically. Third, we perform the test simulations of the CCCP daylighting system using two-dimensional ray-tracing codes. The last, we suggest a new innovative way to estimate the daylighting system's performance; the one-year survey and the performance indexes.

In Chapter 4, we perform a series of simulations of the shape dependence of the CCCP daylighting system. First, we investigate the Mirror I distance dependence and the Mirror II distance dependence. In this section, we can check the effectiveness of our new-type methods to estimate daylighting systems' performance: the one-year survey and the performance indexes. Second, we examine the Mirror I size dependence of the system. Finally, as the results of this chapter, we get the CCCP daylighting system's optimised shape in the range of our simulations.

In Chapter 5, we check the geographic dependence of the CCCP daylighting system using ray-tracing simulations. First, we perform a series of latitude dependence simulations at specific latitudes, and we get the one-year survey sliced by every latitude. Second, we investigate the latitude dependence at noon. Third,

we examine the latitude dependence at summer and winter solstice. The last, we get the detailed performance of the optimised CCCP daylighting system for every latitude.

Throughout the study of this PhD thesis, we can summarise the important results as below (point 1–8):

1.   We introduce a new understandable classification of collectors.

2.   The analytical solution of ODE and geometric analysis clarify the feature of a parabolic mirror.

3.   The CCCP structure is defined and the geometric feature of it is comprehended.

4.   The new-type innovative daylighting system, the CCCP daylighting system, is suggested and investigated the behaviour of it using two-dimensional ray-tracing codes.

5.   To estimate the performance of daylighting systems, the one-year survey, the illuminance rate and the performance indexes are defined.

6.   We examine the dependence of three values that determine the shape of the
      CCCP system and Run 8 gives the optimised shape of the system in the
      range of our simulations as ($\ell_\mathrm{I} = 5.0$, $\ell_\mathrm{II} = 1.0$, $d_\mathrm{I} = 8.0$).

7.   The CCCP daylighting system has two peaks of the illuminance rate under
      $23.45°$ due to the axial tilt of the Earth.

8.   The optimised CCCP daylighting system is available under the latitude of
      $50°$.

These eight items are the major results of this PhD thesis.

6.2   Future Work

In this study, we suggest a new-type revolutionary and innovative daylighting
system, the CCCP system. Moreover, we indicate the performance and usefulness
of the system. However, we have one prominent issue that should be solved.

Chapter 5 indicate the issue. The optimised CCCP daylighting system is

available under 50°. Following the discussion of Chapter 5, the major city in the world is under 65°. We should re-optimise the shape of the CCCP daylighting system that can be available at least under the latitude of 65°.

However, it is not easy to seek the best-optimised shape of the system. To investigate the optimised three values that determine the CCCP system's shape, we run 14 simulations using two-dimensional ray-tracing codes. In our simulations, to get the one-year performance data of each run, we repeat 3,504 times ray-tracing calculation (48 times per day × 73 times per year). We need loads of time to calculate one simulation to investigate one shape of the CCCP daylighting system. Therefore it is not easy to seek by trials and errors.

There are two ways to solve these issues. The first one is a computational solution: to install more vital computer like cluster computing systems and reexamine the codes of ray tracing using like parallel computing. The second one is an analytical solution: to find out the condition that maximises the CCCP daylighting system's performance, formalises such an occasion, and solves the equations.

Both two ways have each advantage and disadvantage. Therefore we need to proceed with two solutions simultaneously. At first, we try analytical formalisation when the CCCP daylighting system is optimised. Moreover, second, for the candidate of the optimised shape, we perform the optimised ray-tracing simulation.

Besides, we have to mention one more solution that is an exciting and disruptive way. When the whole of the CCCP daylighting system rotates against a vertical axis, basically the entire system is rotated against the ground, the performance of the CCCP system is increased. We cannot show the hard evidence of this phenomenon. One of our future work, we investigate the relationship between the rotation and the CCCP daylighting system's performance.

BIBLIOGRAPHY

GORE, A. R. JR. . 2007. *An Inconvenient Truth: The Crisis of Global Warming*. Rodale Press, Pennsylvania.

Hansen, V. G. . *Innovative daylighting systems for deep-plan commercial buildings*. PhD thesis, Queensland University of Technology, 2006.

NAIR, M. G. , RAMAMURTHY, K. , GANESAN, A. R. . 2014. *Classification of indoor daylight enhancement systems*. Lighting Research and Technology, **46**, 245–267.

TANAKA, Y. , SUGANO, S. , SUZUKI, H. . 2012. *A study on daylighting system with parabolic cylinder mirrors*. In 15th International Conference on Geometry and Graphics, Montreal.

SUK, J. Y. , SCHILER, M. , KENSEK, K. . 2017. *Reflectivity and specularity of building*

envelopes: how materiality in architecture affects human visual comfort. Architectural Science Review, **60**(4), 256–265.

TRIPANAGNOSTOPOULOS, Y. , SIABEKOU, CH. , TONUI, J. K. . 2007. *The fresnel lens concept for solar control of buildings.* Solar Energy, **81**, 661–675.

EDMONDS, I. R. GREENUP, P. J. . 2002. *Daylighting in the tropics.* Solar Energy, **73** (2), 111–121.

COURRET, G. , PAULE, B. , SCARTEZZINI, J. L. . 1996. *Anidolic zenithal openings: daylighting and shading.* Lighting Research and Technology, **28**(1), 11–17.

SCARTEZZINI, J. L. COURRET, G. . 2002. *Anidolic daylighting systems.* Solar Energy, **73**(2), 123–135.

ROSEMANN, A. KAASE, H. . 2005. *Lightpipe applications for daylighting systems.* Solar Energy, **78**, 772–780.

ULLAH, I. SHIN, S. . 9 2012. *Development of optical fiber-based daylighting system with uniform illumination.* Journal of the Optical Society of Korea, **16**(3), 247–255.

HECHT, E. . 1998. *Optics.* Addison Wesley Longman, Massachusetts, 3rd edition.

SUZUKI, H. , SUGANO, S. , TOMINAGA, A. . 2015. *Geometric curved line which collimates focusing rays into parallel rays by specular reflection.* In 10th Asian Forum on Graphic Science, page 6.

TSUJI, Y. SUZUKI, H. . 2017. *Evaluating a daylighting system with a convex parabolic reflector.* In 11th Asian Forum on Graphic Science, page 51.

ULLAH, I. SHIN, S. . 2013. *Design of solar lighting system for energy saving.* In International Conference on Modeling and Simulation, Islamabad.

ULLAH, I. WHANG, A. J. W. . 2015. *Development of optical fiber-based daylighting system and its comparison.* Energies, **8**, 7185–7201.

MARDALJEVIC, J. . 2000. *Simulation of annual daylighting profiles for internal illuminance.* Lighting Research and Technology, **32**(3), 111–118.

TSUJI, Y. SUZUKI, H. . 2019. *Geometric feature of a structure composed of concave and convex parabolic mirrors.* Journal for Geometry and Graphics, **23**(2), 235–244.